

April 12, 2024

REGULARIZED METHODS VIA CUBIC MODEL SUBSPACE MINIMIZATION FOR NONCONVEX OPTIMIZATION

STEFANIA BELLAVIA*, DAVIDE PALITTA†, MARGHERITA PORCELLI*,‡, AND
VALERIA SIMONCINI†,§

Abstract. Adaptive cubic regularization methods for solving nonconvex problems need the efficient computation of the trial step, involving the minimization of a cubic model. We propose a new approach in which this model is minimized in a low dimensional subspace that, in contrast to classic approaches, is reused for a number of iterations. Whenever the trial step produced by the low-dimensional minimization process is unsatisfactory, we employ a regularized Newton step whose regularization parameter is a by-product of the model minimization over the low-dimensional subspace. We show that the worst-case complexity of classic cubic regularized methods is preserved, despite the possible regularized Newton steps. We focus on the large class of problems for which (sparse) direct linear system solvers are available and provide several experimental results showing the very large gains of our new approach when compared to standard implementations of adaptive cubic regularization methods based on direct linear solvers. Our first choice as projection space for the low-dimensional model minimization is the polynomial Krylov subspace; nonetheless, we also explore the use of rational Krylov subspaces in case where the polynomial ones lead to less competitive numerical results.

Key words. Adaptive regularization methods, nonconvex optimization, secant methods, Krylov subspaces, worst-case iteration complexity

AMS subject classifications. 49M37, 65K05, 68W40

1. Introduction. We address the numerical solution of possibly nonconvex, unconstrained optimization problems of the form

$$(1.1) \quad \min_{x \in \mathbb{R}^n} f(x),$$

where the objective function $f : \mathbb{R}^n \rightarrow \mathbb{R}$ is supposed to be twice-continuously differentiable and bounded from below. To attack (1.1) we consider second order adaptive regularization methods (AR2). These are well established, globally convergent variants of the Newton method for (1.1), where the step length is implicitly controlled. This feature is achieved by adding a cubic term in the classic quadratic Taylor model to penalize long steps [7, Section 3.3]. More precisely, at a generic AR2 iteration k , the trial step is computed by (approximately) solving the subproblem

$$(1.2) \quad \min_{s \in \mathbb{R}^n} m_k(s),$$

where $m_k(s)$ is the following *cubic regularized model* of the objective function f around the current point x_k

$$(1.3) \quad m_k(s) \stackrel{\text{def}}{=} f(x_k) + s^T \nabla f(x_k) + \frac{1}{2} s^T \nabla^2 f(x_k) s + \frac{1}{3} \sigma_k \|s\|_2^3 = T_k(s) + \frac{1}{3} \sigma_k \|s\|_2^3.$$

The scalar $\sigma_k > 0$ is the regularization parameter and $T_k(s)$ is the second-order Taylor-series expansion of f at x_k .

*Dipartimento di Ingegneria Industriale, Università degli Studi di Firenze, Viale Morgagni, 40/44, 50134 Florence, Italy. Members of the INdAM Research Group GNCS. Emails: {stefania.bellavia,margherita.porcelli}@unifi.it

†Dipartimento di Matematica, (AM)², Alma Mater Studiorum - Università di Bologna, Piazza di Porta San Donato 5, 40126 Bologna, Italia. Members of the INdAM Research Group GNCS. Emails: {davide.palitta,valeria.simoncini}@unibo.it

‡ISTI-CNR, Via Moruzzi 1, Pisa, Italia

§IMATI-CNR, Via Ferrata 5/A, Pavia, Italia

For nonconvex problems, AR2 exhibits a worst-case $\mathcal{O}(\epsilon^{-3/2})$ iteration-complexity to find an ϵ -approximate first-order minimizer, i.e., a point x_ϵ such that

$$(1.4) \quad \|\nabla f(x_\epsilon)\| \leq \epsilon,$$

and a worst-case $\mathcal{O}(\max(\epsilon^{-3/2}, \epsilon_H^{-2}))$ iteration-complexity to find an (ϵ, ϵ_H) -approximate second-order minimizer, i.e., a point x_{ϵ, ϵ_H} such that

$$(1.5) \quad \|\nabla f(x_{\epsilon, \epsilon_H})\| \leq \epsilon \quad \text{and} \quad \lambda_{\min}(\nabla^2 f(x_{\epsilon, \epsilon_H})) \geq -\epsilon_H.$$

AR2 is optimal in terms of complexity when compared to standard second-order methods, such as trust-region and Newton methods, whose iteration-complexity to compute an ϵ -approximate first-order minimizer amounts to $\mathcal{O}(\epsilon^{-2})$ [7, Chapter 3].

The main computational challenge of AR2 procedures is the construction of an approximate solution to (1.2). In the current literature this task is performed either through the solution of the so-called “secular” equation [7, Chapter 9], or by approximately minimizing the cubic model over a sequence of nested Krylov subspaces generated at each nonlinear iteration, onto which the secular equation is projected and solved [7, Chapter 10]. In the first case a sequence of shifted linear systems has to be solved at each nonlinear iteration.

Here we develop a hybrid procedure that combines both the approaches mentioned above for the computation of the trial step. We propose a predictor-corrector scheme, where the prediction step performs the minimization of the cubic model in a low dimensional Krylov subspace, whereas the corrector step, if needed, is a regularized Newton step whose regularization parameter is provided by the prediction step. The subspace is kept *frozen* during the iterations as long as possible; whenever it fails to provide a sufficiently good regularization parameter, the space is *refreshed*, namely a new space is computed. If this new subspace is still unable to provide a good regularization parameter, then an approximate minimizer of the cubic method in the full space is computed by the standard secular-equation-based procedure [7, Chapter 9]. We expect to use this latter step only occasionally.

Our novel scheme is tailored to problems where a factorization of $\nabla^2 f(x_k) + \lambda I$ for a given λ is both feasible and efficient, along the lines of [16]. This is the case for small to medium-sized problems, and also for the large-scale sparse setting; see, e.g. [29]. We chose to employ sparse direct methods for such systems as iterative procedures are highly problem dependent and generally requires a suitable preconditioner. At a first glance, adopting direct solvers for the solution of linear systems may seem in contrast with the construction of Krylov subspaces. Nonetheless, these two strategies are synergic ingredients in our nonlinear optimization solver. Indeed, the minimization of the model over a low-dimensional and possibly frozen Krylov subspace allows us to adaptively adjust the regularization parameter for the regularized Newton step and preserve the complexity of the original AR2, despite a regularized Newton step is possibly employed.

The main practical advantage of our new scheme is the remarkable reduction in the overall number of factorizations of the Hessian matrix, when compared to standard secular-equation-based algorithms as those based on [16]. More precisely, our numerical experiments show that the approximation subspace is refreshed only few times (roughly in the 1.8% of the total number of nonlinear iterations) and the secant method is seldom invoked; see section 6. As a consequence, a significant number of nonlinear iterations sees the computation of at most a single factorization.

Our approach is very general as its derivation does not depend on the chosen reduction space. Nonetheless, the performance can be influenced by this selection. Our first choice is the (classic) polynomial Krylov subspace, which is cheap to construct and performed rather well in our extensive numerical experimentation on different datasets. We also considered using rational Krylov subspaces, which

showed particularly good performance for sequences of slowly varying or severely ill-conditioned subproblems.

Related works. The efficient solution of the subproblem (1.2) in AR2-like methods has been the subject of intense research in the last 20 years; see [7, Chapters 9-10] and references therein. As already mentioned, state-of-the-art methods can be mainly divided into two classes: Approaches based on the approximate minimization of the regularized model using a Lanczos process [6, 18, 19, 23, 26] and schemes based on the secular formulation exploiting matrix factorizations [16]. In [6, 18, 19] the cubic model is minimized over a sequence of nested Krylov subspaces generated by the Lanczos procedure. In [23] it is observed that this approach may produce a large dimensional subspace when applied to ill-conditioned problems and a nested restarting version for the large scale and ill-conditioned case is proposed. Both [23] and [26] reduce the minimization subproblem to a suitable generalized eigenvalue problem.

The algorithm proposed in [15] concurrently solves a set of systems with the shifted Hessian matrix for a predefined large number of shifts by means of a hybrid procedure employing the secular equation combined with the Lanczos method for indefinite linear systems.

A different approach is taken in [5], where the gradient descent is used to approximate the global minimizer of the cubic model; the worst-case iteration complexity is studied.

More recently, several works have focused on the development of modified Newton methods which exhibit the AR2-like worst-case complexity (or nearly so); see e.g. [3, 11, 20]. In [11] a general framework covering several algorithms, like AR2 and the modified trust-region algorithm named TRACE [10], is given. At each iteration the trial step and the multiplier estimate are calculated as an approximate solution of a constrained optimization subproblem whose objective function is a regularized Newton model. A second-order algorithm alternating between a regularized Newton and negative curvature steps is given in [20], while [3] incorporates cubic descent into a quadratic regularization framework.

Similarly to the methods in [3, 11, 20], also our novel scheme employs quadratic-regularization variants preserving the complexity results of the cubic regularization. On the other hand, in contrast to what is done in, e.g., [3, 11], we employ the regularized Newton step only when the step provided by the subspace minimization is not satisfactory. Moreover, the regularization term is a byproduct of the subspace minimization process, and the computation of the smallest eigenvalue of the Hessian matrix is never required when approximate first-order optimality points are sought. We also aim at reducing the computational cost associated to the step computation. To this end, we make use of low dimensional Krylov subspaces whose possibly expensive basis construction is carried out only a handful of times throughout all the nonlinear iterations. Indeed, once a Krylov subspace is constructed at a certain nonlinear iteration k , we reuse it in the subspace minimization as long as possible thus fully capitalizing on the computational efforts performed for its construction. Such a strategy significantly differs from the ones proposed in, e.g., [15, 23, 20, 26].

Outline. Here is a synopsis of the paper. In section 2 we present some preliminary background about the secular formulation of (1.2) (section 2.1) and the AR2 method (section 2.2). Section 3 is devoted to present the main contribution of this paper, namely the novel solution process for (1.1). In section 4 we study the first-order complexity of our algorithm, and show that the optimal worst-case iteration complexity of AR2 is maintained. In section 5 we discuss the choice of the Krylov approximation space. Numerical results displaying the potential of our novel approach are presented in section 6 while in section 7 we draw some conclusions. Finally, Appendix A contains a variant of the proposed algorithm, specifically de-

signed to find approximate second-order optimality points, and the corresponding complexity analysis, while Appendix B collects the complete results obtained during our numerical testing.

Notation. Throughout the paper we adopt the following notation. At the k -th nonlinear iteration, the gradient and the Hessian of f evaluated at the current iterate x_k are denoted as $g_k = \nabla f(x_k)$ and $H_k = \nabla^2 f(x_k)$, respectively. The symbol I is used for the $n \times n$ identity matrix, and $\|\cdot\|$ denotes the Euclidean norm of a vector.

2. Preliminaries. This section provides a brief description of the features of the cubic regularized minimization problem (1.2) in terms of its secular formulation and a quick review of the main steps of the AR2 method.

2.1. The “secular” formulation. The secular formulation of the subproblem (1.2) is defined by exploiting the characterization of the global minimizer of $m_k(s)$ reported below. For the sake of simplicity, in this section we omit the subscript k .

THEOREM 2.1. [7, Theorem 8.2.8] *Any global minimizer s^* of (1.2) satisfies*

$$(2.1) \quad (H + \lambda^* I)s^* = -g,$$

where $H + \lambda^* I$ is positive semidefinite and

$$\lambda^* = \sigma \|s^*\|.$$

If $H + \lambda^* I$ is positive definite, then s^* is unique.

Let λ_1 be the leftmost eigenvalue of H . In the so-called “easy case”, $\lambda^* > \lambda_S \stackrel{\text{def}}{=} \max\{0, -\lambda_1\}$ and a solution to (1.2) can be computed by solving the scalar *secular equation*

$$(2.2) \quad \phi_R(\lambda; g, H, \sigma) \stackrel{\text{def}}{=} \|(H + \lambda I)^{-1}g\| - \frac{\lambda}{\sigma} = 0.$$

It can be proved that the Newton and the secant methods applied to (2.2) rapidly converge to λ^* starting from any approximation in $(\lambda_S, +\infty)$ [6, 7, 16]. Whenever the computation of λ_1 is prohibitive and the computation of appropriate starting guesses is thus not guaranteed, suitable estimations to λ_1 can be derived as done in [16].

As opposite to the “easy case”, the “hard case” takes place when $\lambda_1 < 0$ and g is orthogonal to the λ_1 -eigenspace of H , namely $v^T g = 0$ for all v in $\{v : (H - \lambda_1 I)v = 0\}$. In this case, $\lambda^* = -\lambda_1$ and there is no solution to the secular equation in $(\lambda_S, +\infty)$. Sophisticated numerical strategies have to be employed to compute the global minimizer s^* in this case; see, e.g., [7, Section 9.3.4].

The theorem below summarizes the form of the global minimizer of (1.2) in both the easy and the hard cases.

THEOREM 2.2. [7, Corollary 8.3.1] *Any global minimizer of (1.2) can be expressed as*

$$(2.3) \quad s^* = \begin{cases} -(H + \lambda^* I)^{-1}g \text{ (uniquely)} & \text{if } \lambda^* > -\lambda_1, \\ -(H + \lambda^* I)^\dagger g + \alpha v_1 & \text{if } \lambda^* = -\lambda_1, \end{cases}$$

where $(H + \lambda^* I)^\dagger$ denotes the pseudoinverse of $H + \lambda^* I$, $\lambda^* = \sigma \|s^*\|$, λ_1 is the leftmost eigenvalue of H , v_1 is any corresponding eigenvector, and α is one of the two roots of $\|-(H + \lambda^* I)^\dagger g + \alpha v_1\| = \lambda^* / \sigma$.

Algorithm 2.1 The adaptive-regularization algorithm with a second order model (AR2) algorithm [7]

Require: An initial point x_0 ; accuracy threshold $\epsilon \in (0, 1)$; an initial regularization parameter $\sigma > 0$ are given as well as constants $\eta_1, \eta_2, \gamma_1, \gamma_2, \theta_1, \sigma_{\min}$ that satisfy

$$\sigma_{\min} \in (0, \sigma_0], \quad \theta_1 > 0, \quad 0 < \eta_1 \leq \eta_2 < 1, \quad 0 < \gamma_1 < 1 < \gamma_2.$$

- 1: Compute $f(x_0), g_0 = \nabla f(x_0), H_0 = \nabla^2 f(x_0)$, and set $k = 0$.
- 2: **Step 1: Test for termination.** If $\|g_k\| \leq \epsilon$, terminate.
- 3: **Step 2: Step computation.** Compute a step s_k such that

$$(2.5) \quad m_k(s_k) < m_k(0)$$

and

$$(2.6) \quad \|\nabla m_k(s_k)\| \leq \frac{1}{2}\theta_1\|s_k\|^2$$

- 4: **Step 3: Acceptance of the trial point.** Compute $f(x_k + s_k)$ and the ratio ρ_k given in (2.4).
- 5: If $\rho_k \geq \eta_1$, then define $x_{k+1} = x_k + s_k$ and compute $g_{k+1} = \nabla f(x_{k+1})$ and $H_{k+1} = \nabla^2 f(x_{k+1})$. Otherwise define $x_{k+1} = x_k$.
- 6: **Step 4: Regularization parameter update.** Compute

$$(2.7) \quad \sigma_{k+1} \in \begin{cases} [\max(\sigma_{\min}, \gamma_1\sigma_k), \sigma_k] & \text{if } \rho_k \geq \eta_2 \\ \sigma_k & \text{if } \rho_k \in [\eta_1, \eta_2) \\ \gamma_2\sigma_k & \text{otherwise} \end{cases}$$

- 7: Increment k by one and **goto** Step 1.
-

2.2. The AR2 method. The AR2 method is an iterative procedure where, at iteration k , a trial step s_k is computed by approximately minimizing the cubic model (1.3). Algorithm 2.1 summarizes a possible implementation of the AR2 algorithm; see also [7, Algorithm 3.3.1]. Theorem 2.2 determines the exact minimizer of $m_k(s)$ but, in practice, only an approximate minimizer s_k satisfying conditions (2.5) and (2.6) in Algorithm 2.1 is indeed necessary; see, e.g., [7, p.65].

Given the trial step s_k , the trial point $x_k + s_k$ is then used to compute the ratio

$$(2.4) \quad \rho_k = \frac{f(x_k) - f(x_k + s_k)}{T_k(0) - T_k(s_k)},$$

with T_k as in (1.3). If $\rho_k \geq \eta_1$, with $\eta_1 \in (0, 1)$, then the trial point is accepted, the iteration is declared successful and the regularization parameter σ_k is possibly decreased. Otherwise, an unsuccessful iteration occurs: The point $x_k + s_k$ is rejected and the regularisation parameter is increased.

3. The new FAR2 algorithm. In this section we introduce our subspace cubic approach that we name the Frozen AR2 (FAR2) algorithm. The main idea behind FAR2 is to construct a low-dimensional subspace \mathcal{K} at the initial iteration, compute a minimizer to the cubic model projected onto this subspace, and then keep using such subspace also in the subsequent nonlinear iterations. The minimizer of $m_k(s)$ over \mathcal{K} is cheaply computed by solving the *projected* secular equation, that is equation (2.2) where the quantities involved H and g consist of the projection of H_k and g_k onto \mathcal{K} , respectively. If (2.6) in Algorithm 2.1 is not satisfied by such

minimizer¹, then a further regularized Newton-like step is performed where the employed regularization parameter $\widehat{\lambda}_k$ is a by-product of the minimization process over the current subspace. The current subspace \mathcal{K} is discarded and a new, more informative approximation space is generated whenever either the computed $\widehat{\lambda}_k$ does not provide a regularized Newton step s_k such that

$$(3.1) \quad s_k^T (H_k + \widehat{\lambda}_k I) s_k > 0,$$

or s_k fails to satisfy the following condition:

$$(3.2) \quad C_{\text{low}} \|\widehat{s}_k\| \leq \|s_k\| \leq C_{\text{up}} \|\widehat{s}_k\|,$$

where \widehat{s}_k is the minimizer of the cubic model onto the current subspace and C_{low} and C_{up} are given positive constants.

Notice that condition (3.1) is significantly less restrictive than requiring $H_k + \widehat{\lambda}_k I$ positive definite [20]. Moreover, condition (3.2) will be crucial to analyze the complexity of FAR2 in section 4 and is similar to the one adopted in [11, Eq. (2.1)]. Note that condition (3.2) is not restrictive as it only requires that the ratio $\|s_k\|/\|\widehat{s}_k\|$ is lower bounded away from zero and upper bounded.

The overall FAR2 procedure is described in Algorithm 3.1 and Algorithm 3.2. The outcomes of Algorithm 3.2 are the regularization parameter $\widehat{\lambda}_k$, the step \widehat{s}_k , the matrix W_k storing the basis of the subspace used to carry out the minimization process needed to generate $\widehat{\lambda}_k$ and \widehat{s}_k . The matrix W_k is such that $\text{Range}(W_k) = \text{Range}([g_k, V_{k+1}])$. The columns of the matrix V_{k+1} represent an orthonormal basis of the current subspace \mathcal{K} and they are computed from scratch whenever the input parameter **refresh** is equal to one. The minimization is carried out over the augmented subspace spanned by W_k to exactly project the current gradient g_k . The input parameter $j_{\text{max}} \ll n$ rules the maximum allowed dimension of the subspace spanned by V_{k+1} .

The reduced step \widehat{s}_k is the exact global minimizer of $m_k(s)$ onto the subspace generated by W_k . Moreover, the regularization parameter has the following form:

$$(3.4) \quad \widehat{\lambda}_k = \sigma_k \|\widehat{s}_k\|.$$

In Line 4 of Algorithm 3.1 the minimizer \widehat{s}_k of the cubic model onto the current subspace and the regularization parameter $\widehat{\lambda}_k$ are computed by invoking Algorithm 3.2. If $W_k \widehat{s}_k$ satisfies (2.6), we set $s_k = W_k \widehat{s}_k$ and proceed with Step 3 while the current \mathcal{K} is kept frozen. Otherwise, in Line 8, the regularized Newton step $s_k = -(H_k + \widehat{\lambda}_k I)^{-1} g_k$ is computed and used in Step 3 whenever the conditions (3.1) and (3.2) hold. If one of these conditions is not satisfied, s_k is rejected. In this scenario the current subspace is refreshed if it comes from previous iterations and the subspace minimization strategy is attempted once again. Otherwise, namely if \mathcal{K} has just been refreshed, a new step s_k satisfying (2.5)-(2.6) is computed by approximately solving the secular equation $\phi_R(\lambda; g_k, H_k, \sigma_k) = 0$. The latter equation is solved (see (2.2)) by the secant method ([16] and [7, Chapter 9]) equipped with suitable stopping criteria; see [7, Theorem 9.3.2]. The flag **refresh** rules the computation of a new subspace. A new subspace is computed whenever **refresh** is 1. The flag **refresh** is set to 1 at the first iteration and whenever the following situation occurs

- ♣ **refresh** is currently set to 0, the minimization of the model in the current subspace does not satisfy (2.6), and either (3.1) or (3.2) does not hold.

One iteration is declared unsuccessful when ♣ occurs or, as in classic adaptive methods, when the ratio ρ_k in (2.4) is smaller than the input parameter $\eta_1 \in (0, 1)$.

¹Condition (2.5) is naturally satisfied as the null vector lies in such subspace.

Algorithm 3.1 The Frozen AR2 (FAR2) algorithm

Require: An initial point x_0 ; accuracy threshold $\epsilon \in (0, 1)$; an initial regularization parameter $\sigma_0 > 0$ are given, and constants $\eta_1, \eta_2, \gamma_1, \gamma_2, \theta_1, \sigma_{\min}$ s.t.

$$\sigma_{\min} \in (0, \sigma_0], \theta_1 > 0, 0 < \eta_1 \leq \eta_2 < 1, 0 < \gamma_1 < 1 < \gamma_2, 0 < C_{\text{low}} < C_{\text{up}}$$

An integer $j_{\max} \ll n$.

- 1: Compute $f(x_0), g_0 = \nabla f(x_0), H_0 = \nabla^2 f(x_0)$, and set $k = 0$, **refresh** = 1 and $V_0 = []$.
- 2: **Step 1: Test for termination.** If $\|g_k\| \leq \epsilon$, terminate.
- 3: **Step 2: Step computation.**
- 4: Invoke Algorithm 3.2 providing the scalar $\hat{\lambda}_k$, the reduced step \hat{s}_k , the basis W_k and V_{k+1}
- 5: **if** $W_k \hat{s}_k$ satisfies (2.6)
- 6: set $s_k = W_k \hat{s}_k$ and **goto** Step 3
- 7: **end if**
- 8: Compute $s_k = -(H_k + \hat{\lambda}_k I)^{-1} g_k$. % regularized Newton step
- 9: **if** $s_k^T (H_k + \hat{\lambda}_k I) s_k \leq 0$ or $\|s_k\| / \|\hat{s}_k\| < C_{\text{low}}$ or $\|s_k\| / \|\hat{s}_k\| > C_{\text{up}}$
- 10: **if refresh**
- 11: Find λ_k and $s_k = -(H_k + \lambda_k I)^{-1} g_k$ such that (2.5)-(2.6) hold by applying the secant method to $\phi_R(\lambda_k; g_k, H_k, \sigma_k) = 0$
- 12: **Goto** Step 3
- 13: **else**
- 14: Define $x_{k+1} = x_k, \sigma_{k+1} = \sigma_k$, set **refresh** = 1, $k = k + 1$
- 15: **Goto** Step 1 % unsuccessful iteration, step rejection
- 16: **end if**
- 17: **Step 3:** Compute

$$\rho_k = \frac{f(x_k) - f(x_k + s_k)}{T_k(0) - T_k(s_k)}.$$

- 18: **Step 4:**
- 19: **if** $\rho_k \geq \eta_1$ **then** % Successful iteration
- 20: set $x_{k+1} = x_k + s_k$, compute $g_{k+1} = \nabla f(x_{k+1}), H_{k+1} = \nabla^2 f(x_{k+1})$
- 21: **else** % unsuccessful iteration, step rejection
- 22: set $x_{k+1} = x_k$
- 23: **end if**
- 24: **Step 5: Regularization parameter update.** Compute

$$(3.3) \quad \sigma_{k+1} \in \begin{cases} [\max\{\sigma_{\min}, \gamma_1 \sigma_k\}, \sigma_k] & \text{if } \rho_k \geq \eta_2 \\ \sigma_k & \text{if } \rho_k \in [\eta_1, \eta_2) \\ \gamma_2 \sigma_k & \text{otherwise} \end{cases}$$

- 25: Increment k by one, set **refresh** = 0 and **goto** Step 1.
-

Note that, in case of ♣, the parameter σ_k is left unchanged and a new subspace is computed at the subsequent iteration. We refrain from increasing σ_k in this case as the failure is not ascribed to an unsatisfactory model but rather to a poor subspace. On the contrary, in case the unsuccessful iteration is due to $\rho_k < \eta_1$, the parameter σ_k is increased. The flag **refresh** is set to 0 in Step 5 as this step is executed only if either (2.6) holds or both (3.1) and (3.2) are satisfied. In this case we keep \mathcal{K} frozen.

We observe that when the condition in Line 5 of Algorithm 3.2 is met, that is when the subspace minimization provides a reduced step \hat{s}_k such that $W_k \hat{s}_k$ satis-

Algorithm 3.2 Minimization of m_k over the low-dimensional subspace

Require: The matrix H_k ; the vector g_k ; the matrix $V_k \in \mathbb{R}^{n \times d_k}$; the accuracy threshold $\theta_1 > 0$; the parameter σ_k ; an integer $j_{\max} \ll n$; **refresh**.

```

1:   if refresh                                     % Generate new proj space
2:       Set  $V_{k+1} = []$ 
3:       for  $j = 1, \dots, j_{\max} - 1$ 
4:           Set2  $W^{(j)} = \text{orth}([V_{k+1}, g_k])$ 
5:           Compute projections  $g^{(j)} = (W^{(j)})^T g_k$ ,  $H^{(j)} = (W^{(j)})^T H_k W^{(j)}$ 
6:           Find  $\hat{\lambda}$  s.t.  $\phi_R(\hat{\lambda}; g^{(j)}, H^{(j)}, \sigma_k) = 0$ , i.e.
                                     
$$\hat{\lambda} = \sigma_k \|(H^{(j)} + \hat{\lambda}I)^{-1} g^{(j)}\|$$

7:           Set  $\hat{s} = -(H^{(j)} + \hat{\lambda}I)^{-1} g^{(j)}$ 
8:           if  $\|\nabla m_k(W^{(j)} \hat{s})\| \leq \frac{1}{2} \theta_1 \|\hat{s}\|^2$ 
9:               Set  $\hat{\lambda}_k = \hat{\lambda}$ ,  $\hat{s}_k = \hat{s}$ ,  $W_k = W^{(j)}$  and return
10:          end if
11:          Expand  $V_{k+1}$  with new basis vector
12:       end for
13:       Set  $\hat{\lambda}_k = \hat{\lambda}$ ,  $\hat{s}_k = \hat{s}$ ,  $W_k = W^{(j)}$  and return
14:   else                                           % Project onto the old space
15:       Set  $W^{(\hat{j})} = \text{orth}([V_k, g_k])$ , where  $\hat{j} = d_k + 1$ 
16:       Compute projections  $g^{(\hat{j})} = (W^{(\hat{j})})^T g_k$ ,  $H^{(\hat{j})} = (W^{(\hat{j})})^T H_k W^{(\hat{j})}$ 
17:       Find  $\hat{\lambda}$  s.t.  $\phi_R(\hat{\lambda}; g^{(\hat{j})}, H^{(\hat{j})}, \sigma_k) = 0$ , i.e.
                                     
$$\hat{\lambda} = \sigma_k \|(H^{(\hat{j})} + \hat{\lambda}I)^{-1} g^{(\hat{j})}\|$$

18:       Set  $\hat{s}_k = -(H^{(\hat{j})} + \hat{\lambda}I)^{-1} g^{(\hat{j})}$ ,  $\hat{\lambda}_k = \hat{\lambda}$ 
19:       Set  $V_{k+1} = V_k$  and  $W_k = W^{(\hat{j})}$ 
20:   end if

```

fies (2.6), then the computation of the regularized Newton step and the consequent factorization of the shifted Hessian matrix in the full space are not needed.

We would like to point out the different nature of the step s_k in the successful iterations. If the step is computed in Line 6 of Algorithm 3.1, then it is such that (2.6) holds and $\|s_k\| = \|\hat{s}_k\|$ since W_k has orthonormal columns. On the other hand, if it is computed in Line 8 of Algorithm 3.1, it ensures a decrease of the quadratic regularized model

$$(3.5) \quad m_k^Q(s) \stackrel{\text{def}}{=} T_k(s) + \frac{1}{2} \hat{\lambda}_k \|s\|^2,$$

with $\hat{\lambda}_k = \sigma_k \|\hat{s}_k\|$, as the following inequality holds:

$$(3.6) \quad m_k^Q(s_k) = T_k(s_k) + \frac{1}{2} \sigma_k \|\hat{s}_k\| \|s_k\|^2 < m_k^Q(0).$$

Indeed,

$$(3.7) \quad m_k^Q(s_k) = f_k + s_k^T g_k + \frac{1}{2} s_k^T (H_k + \hat{\lambda}_k I) s_k,$$

and by (3.1) and $s_k^T (H_k + \hat{\lambda}_k I) s_k = -s_k^T g_k$, we get

$$(3.8) \quad m_k^Q(s_k) - m_k^Q(0) = s_k^T g_k - \frac{1}{2} s_k^T g_k = \frac{1}{2} s_k^T g_k < 0.$$

²Here and in the following, `orth` defines a procedure that updates a matrix having orthonormal columns by adding a new column and orthogonalizing it with respect to the previous ones.

Note that, in case $H_k + \widehat{\lambda}_k I$ is positive definite, the step s_k is the exact global minimizer of the quadratic regularized model $m_k^Q(s)$.

When s_k is computed in Line 11 of Algorithm 3.1 it is still an approximate minimizer of the cubic model satisfying (2.5)-(2.6).

We finally stress that condition (3.2) holds whenever there exist $0 < \theta_{\min} < \theta_{\max}$ such that $\lambda_i(H_k + \widehat{\lambda}_k I)^{-2} \in [\theta_{\min}, \theta_{\max}]$, for $i = 1, \dots, n$. Indeed, we have

$$\|s_k\|^2 = g_k^T (H_k + \widehat{\lambda}_k I)^{-2} g_k,$$

so that

$$\theta_{\min} \|g_k\|^2 \leq \|s_k\|^2 \leq \theta_{\max} \|g_k\|^2.$$

Similarly, since g_k is always included in the subspace employed to compute \widehat{s}_k , it holds

$$\widehat{\theta}_{\min} \|g_k\|^2 \leq \|\widehat{s}_k\|^2 \leq \widehat{\theta}_{\max} \|g_k\|^2,$$

where $\widehat{\theta}_{\min}$ and $\widehat{\theta}_{\max}$ denote the smallest and largest eigenvalues of $(\widehat{H}_k + \widehat{\lambda}_k I)^{-2}$, respectively. Notice that $\widehat{\theta}_{\min}$ and $\widehat{\theta}_{\max}$ are guaranteed to be strictly positive as $\widehat{\lambda}_k$ solves the reduced secular equation so that $\widehat{H}_k + \widehat{\lambda}_k I$ is certainly positive definite. Therefore,

$$\|g_k\|^2 \leq \frac{\|\widehat{s}_k\|^2}{\widehat{\theta}_{\min}}, \quad \frac{\|\widehat{s}_k\|^2}{\widehat{\theta}_{\max}} \leq \|g_k\|^2.$$

By putting everything together, we have

$$\frac{\theta_{\min}}{\theta_{\max}} \|\widehat{s}_k\|^2 \leq \|s_k\|^2 \leq \frac{\theta_{\max}}{\theta_{\min}} \|\widehat{s}_k\|^2.$$

4. Complexity analysis of finding first-order optimality points. Given $\epsilon > 0$ we provide an upper bound on the number of iterations needed by FAR2 to compute an ϵ -approximate first-order optimality point (see (1.4)). To this end, we make the following standard assumptions on the optimization problem (1.1).

- AS.1** $f(x)$ is twice continuously differentiable in \mathbb{R}^n , and its gradient $\nabla f(x)$ and its Hessian $\nabla^2 f(x)$ are Lipschitz continuous on \mathbb{R}^n with Lipschitz constants L_1 and L_2 , respectively.
- AS.2** $f(x)$ is bounded from below in \mathbb{R}^n , that is there exists a constant f_{low} such that $f(x) \geq f_{\text{low}}$ for all $x \in \mathbb{R}^n$.

We recall that, given $x_k, s_k \in \mathbb{R}^n$ and by letting $T_k(s_k)$ be the second-order Taylor approximation of $f(x_k + s_k)$ around x_k , Assumption **AS.1** implies the following

$$(4.1) \quad |f(x_k + s_k) - T_k(s_k)| \leq \frac{L_2}{6} \|s_k\|^3,$$

see, e.g., [7, Corollary A.8.4].

Let us denote by \mathcal{I}_{RN} the set of indexes of iterations such that the step s_k used in Step 3 has been computed in Line 8 of Algorithm 3.1, i.e., it is a regularized Newton step. We observe that at any successful iteration $k \notin \mathcal{I}_{RN}$ the step s_k is the step used in the classic adaptive regularization method³ employing the second order model. Then, we can rely on the theoretical results given in [7, Section 3.3] for these iterations and prove analogous results for iterations in \mathcal{I}_{RN} . Our analysis follows the classic path for proving worst-case complexity of adaptive regularized methods despite a regularized Newton step is used. We also observe that condition (3.2)

³It is an approximate minimizer satisfying (2.5)-(2.6) both when it is computed in Line 6 and in Line 11.

holds at any successful iteration $k \in \mathcal{I}_{RN}$ and that, as already noticed, σ_k is left unchanged at any unsuccessful iteration in \mathcal{I}_{RN} where (3.2) does not hold.

We are now going to establish a key lower bound on the Taylor-series model decrease. In case $k \notin \mathcal{I}_{RN}$, the classic lower-bound of AR2 methods holds. Remarkably, the lower bound depends on $\|s_k\|^3$ also for $k \in \mathcal{I}_{RN}$ provided that (3.2) holds. This lower bound is crucial to prove the optimal complexity of our procedure and it holds as $\hat{\lambda}_k$ is the minimizer of the cubic model in the low-dimensional subspace yielding $\hat{\lambda}_k = \sigma_k \|\hat{s}_k\|$.

LEMMA 4.1. (Decrease in the Taylor-series model) *At every successful iteration k of the FAR2 algorithm, it holds that*

$$(4.2) \quad T_k(0) - T_k(s_k) > \frac{1}{2} \sigma_k \|\hat{s}_k\| \|s_k\|^2, \quad \text{for } k \in \mathcal{I}_{RN},$$

and

$$(4.3) \quad T_k(0) - T_k(s_k) > \frac{1}{3} \sigma_k \|s_k\|^3, \quad \text{for } k \notin \mathcal{I}_{RN}.$$

Proof. Let us consider the case $k \in \mathcal{I}_{RN}$. Inequality (3.6) yields

$$T_k(0) - T_k(s_k) = m_k^Q(0) - m_k^Q(s_k) + \frac{1}{2} \sigma_k \|\hat{s}_k\| \|s_k\|^2 \geq \frac{1}{2} \sigma_k \|\hat{s}_k\| \|s_k\|^2.$$

In case $k \notin \mathcal{I}_{RN}$, the result follows from [7, Lemma 3.3.1]. \square

LEMMA 4.2. (Upper bound on the regularization parameter) *Suppose that Assumption AS.1 holds. At each iteration of the FAR2 algorithm it holds*

$$(4.4) \quad \sigma_k \leq \sigma_{\max} \stackrel{\text{def}}{=} \max \left\{ \sigma_0, \gamma_2 \frac{L_2 C_{\text{up}}}{3(1-\eta_1)}, \gamma_2 \frac{L_2}{2(1-\eta_1)} \right\},$$

where γ_2 and η_1 are given in the algorithm.

Proof. For any $k \notin \mathcal{I}_{RN}$, by exploiting (4.3) and proceeding as in [7, Lemma 3.3.2] we can show that the iteration is successful whenever

$$\sigma_k \geq \frac{L_2}{2(1-\eta_1)}.$$

In case $k \in \mathcal{I}_{RN}$ the following two situations can occur:

- a) Both conditions (3.1) and (3.2) hold.
- b) Either (3.1) or (3.2) does not hold. The iteration is declared unsuccessful in Line 14 of Algorithm 3.1. `refresh` is set to 1 and σ_k is left unchanged.

Let us consider case a). The ratio ρ_k is evaluated in Step 5 and from its definition we have

$$\begin{aligned} |\rho_k - 1| &= \frac{|f(x_k) - f(x_k + s_k) - T_k(0) + T_k(s_k)|}{T_k(0) - T_k(s_k)} \\ &= \frac{|f(x_k + s_k) - T_k(s_k)|}{T_k(0) - T_k(s_k)} \\ &\leq \frac{L_2 \|s_k\|^3}{3\sigma_k \|\hat{s}_k\| \|s_k\|^2} \\ &= \frac{L_2 \|s_k\|}{3\sigma_k \|\hat{s}_k\|}, \end{aligned}$$

where we used the inequalities (4.1) and (4.2). Therefore, by using (3.2), we can conclude that if $k \in \mathcal{I}_{RN}$ and case a) occurs, then

$$\sigma_k \geq \frac{L_2 C_{\text{up}}}{3(1-\eta_1)},$$

which implies $\rho_k > \eta_1$, i.e., the iteration is successful. Therefore, thanks to the mechanism of the algorithm we have

$$\sigma_k \leq \gamma^2 \frac{L_2 C_{\text{up}}}{3(1 - \eta_1)},$$

for any $k \in \mathcal{I}_{RN}$ such that case **a**) holds.

Finally, unsuccessful iterations $k \in \mathcal{I}_{RN}$ such that case **b**) holds do not yield an increase in σ_k .

Therefore, σ_k cannot be larger than σ_{\max} , and the bound in (4.4) follows. \square

We are now going to show two crucial properties that provide the optimal complexity result.

LEMMA 4.3. *Suppose that Assumption **AS.1** holds. Then, at any successful iteration k of the FAR2 algorithm, if $k \in \mathcal{I}_{RN}$ then*

$$\|\widehat{s}_k\|^2 \geq \frac{2}{C_{\text{up}}(L_1 C_{\text{up}} + 2\sigma_{\max})} \|g_{k+1}\|.$$

Moreover, at any successful iteration, the following inequality holds

$$(4.5) \quad f(x_k) - f(x_{k+1}) \geq \eta_1 \sigma_{\min} \min \left\{ \frac{1}{2} C_{\text{low}}^2 \kappa_0, \frac{1}{3} \kappa_1 \right\} \|g_{k+1}\|^{3/2},$$

$$\text{where } \kappa_0 = \left(\frac{2}{C_{\text{up}}(L_1 C_{\text{up}} + 2\sigma_{\max})} \right)^{3/2}, \quad \kappa_1 = \left(\frac{2}{L_1 + \theta_1 + \sigma_{\max}} \right)^{3/2}.$$

Proof. Let us consider the case $k \in \mathcal{I}_{RN}$. By using the definition of s_k in Line 8 of Algorithm 3.1, (3.2), (4.4), and the form of λ_k given in (3.4), it follows that

$$(4.6) \quad \begin{aligned} \|g_{k+1}\| &\leq \|g_{k+1} - (H_k s_k + g_k)\| + \|H_k s_k + g_k\| \\ &\leq \frac{L_1}{2} \|s_k\|^2 + \sigma_k \|\widehat{s}_k\| \|s_k\| \\ &\leq C_{\text{up}} \left(\frac{L_1}{2} C_{\text{up}} + \sigma_{\max} \right) \|\widehat{s}_k\|^2. \end{aligned}$$

Then, (4.2) yields

$$\begin{aligned} f(x_k) - f(x_{k+1}) &\geq \eta_1 (T_k(0) - T_k(s_k)) \\ &\geq \frac{\eta_1}{2} \sigma_k \|\widehat{s}_k\| \|s_k\|^2 \geq \frac{\eta_1}{2} \sigma_{\min} C_{\text{low}}^2 \|\widehat{s}_k\|^3 \\ &\geq \frac{\eta_1}{2} \sigma_{\min} C_{\text{low}}^2 \kappa_0 \|g_{k+1}\|^{3/2}, \end{aligned}$$

$$\text{where } \kappa_0 \stackrel{\text{def}}{=} \left(\frac{2}{C_{\text{up}}(L_1 C_{\text{up}} + 2\sigma_{\max})} \right)^{3/2}.$$

In case $k \notin \mathcal{I}_{RN}$, Lemma 3.3.3 in [7] ensures that the step s_k computed in Line 6 of Algorithm 3.1 satisfies:

$$\|g_{k+1}\| \leq \frac{L_1 + \theta_1 + \sigma_{\max}}{2} \|s_k\|^2,$$

and from (4.3) it follows that

$$f(x_k) - f(x_{k+1}) \geq \eta_1 (T_k(0) - T_k(s_k)) \geq \eta_1 \frac{1}{3} \sigma_k \|s_k\|^3 \geq \eta_1 \frac{1}{3} \sigma_{\min} \kappa_1 \|g_{k+1}\|^{3/2},$$

$$\text{where } \kappa_1 \stackrel{\text{def}}{=} \left(\frac{2}{L_1 + \theta_1 + \sigma_{\max}} \right)^{3/2}. \quad \square$$

Let us denote by \mathcal{S}_k the set of indexes of successful iterations up to iteration k generated by the FAR2 method detailed in Algorithms 3.1-3.2. Then, the following result allows us to bound the number of iterations in terms of the number of successful iterations provided that the regularization parameter is bounded from above.

LEMMA 4.4. *Suppose that the sequence $\{x_k\}$ is generated by the FAR2 algorithm. Assume that $\sigma_k \leq \sigma_{\max}$ for some $\sigma_{\max} > 0$. Then,*

$$k \leq \left(|\mathcal{S}_k| \left(3/2 + \frac{3/2 |\log \gamma_1|}{\log \gamma_2} \right) + \frac{3/2}{\log \gamma_2} \log \left(\frac{\sigma_{\max}}{\sigma_0} \right) \right).$$

Proof. Let $\mathcal{U}_{k,1}$ and $\mathcal{U}_{k,2}$ be the sets of indexes of the iterations declared unsuccessful in Step 4 and in Line 14 up to iteration k generated by the FAR2 algorithm, respectively. Observe that in case $j \in \mathcal{U}_{k,2}$, $\sigma_{j+1} = \sigma_j$. Then, by proceeding as in [7, Lemma 2.4.1] we easily get that

$$|\mathcal{U}_{k,1}| + |\mathcal{S}_k| \leq |\mathcal{S}_k| \left(1 + \frac{|\log \gamma_1|}{\log \gamma_2} \right) + \frac{1}{\log \gamma_2} \log \left(\frac{\sigma_{\max}}{\sigma_0} \right).$$

Since `refresh` is set to 1 at any iteration in $\mathcal{U}_{k,2}$ and we can have an iteration in $\mathcal{U}_{k,2}$ only with `refresh`=0, it follows that we can have at most one iteration in $\mathcal{U}_{k,2}$ every two iterations in $\mathcal{U}_{k,1} \cup \mathcal{S}_k$. Then, the result follows. \square

We can now resort to the standard “telescoping sum” argument to prove the following iteration complexity result showing that FAR2 preserves the optimal complexity of AR2.

THEOREM 4.5. *Suppose that **AS.1** and **AS.2** hold. Given $\epsilon \in (0, 1)$, there exists a constant κ_p such that the FAR2 algorithm needs at most*

$$\left\lceil \frac{f(x_0) - f_{\text{low}}}{\kappa_p} \epsilon^{-\frac{3}{2}} + 1 \right\rceil,$$

successful iterations and at most

$$\left(\left\lceil \frac{f(x_0) - f_{\text{low}}}{\kappa_p} \epsilon^{-\frac{3}{2}} + 1 \right\rceil \left(3/2 + \frac{3/2 |\log \gamma_1|}{\log \gamma_2} \right) + \frac{3/2}{\log \gamma_2} \log \left(\frac{\sigma_{\max}}{\sigma_0} \right) \right),$$

iterations to compute an iterate x_k such that $\|g_k\| \leq \epsilon$.

Proof. At each successful iteration k the algorithm guarantees the decrease in (4.5). Then,

$$(4.7) \quad f(x_k) - f(x_{k+1}) \geq \eta_1 \sigma_{\min} \min \left\{ \frac{1}{2} C_{\text{low}}^2 \kappa_0, \frac{1}{3} \kappa_1 \right\} \epsilon^{3/2},$$

whenever $\|g_{k+1}\| > \epsilon$. Thus, letting \bar{k} such that $\bar{k} + 1$ is the first iteration where $\|g_{\bar{k}+1}\| \leq \epsilon$ and summing up from $k = 0$ to $\bar{k} - 1$, since $f(x_k) = f(x_{k+1})$ along unsuccessful iterations, and using the telescopic sum property, we obtain

$$f(x_0) - f(x_{\bar{k}}) \geq \kappa_p \epsilon^{\frac{3}{2}} |\mathcal{S}_{\bar{k}-1}|,$$

where $\kappa_p = \eta_1 \sigma_{\min} \min \left\{ \frac{1}{2} C_{\text{low}}^2 \kappa_0, \frac{1}{3} \kappa_1 \right\}$.

Since f is bounded from below by f_{low} , we conclude that

$$(4.8) \quad |\mathcal{S}_{\bar{k}}| \leq \frac{f(x_0) - f_{\text{low}}}{\kappa_p} \epsilon^{-\frac{3}{2}} + 1.$$

Lemma 4.4 then yields the upper bound on the total number of iterations. \square

REMARK 4.1. Given $\epsilon, \epsilon_H > 0$, Algorithm 3.1 can be suitably modified in order to compute an (ϵ, ϵ_H) -approximate second-order minimizer (see (1.5)). We will refer to this variant of FAR2 as *Frozen AR2-Second Order* (FAR2-SO) and the corresponding algorithms are detailed in Appendix A (Algorithm A.1 and Algorithm A.2), together with a complexity analysis.

5. Choice of the approximation space. The performance of Algorithm 3.1 strongly depends on the chosen approximation space $\mathcal{K}_{d_k} = \text{Range}(V_k)$ used for projecting the problem. The construction of the approximation space and the definition of the related projected quantities are handled by Algorithm 3.2. The latter is given in full generality, regardless of the nature of $\text{Range}(V_k)$. However, some of its steps simplify according to the adopted subspace, as illustrated in the following. Moreover, the performance of Algorithm 3.1 largely benefits from the inclusion of the current g_k in the approximation space. In particular, the exact representation of g_k in the space is crucial for obtaining the bounds on $\|s_k\|$ reported in (3.2).

In our framework, we define $V_k \in \mathbb{R}^{n \times d_k}$ as an orthonormal basis of the polynomial Krylov subspace generated at iteration d_k of Algorithm 3.2, by the current H_k and g_k , namely

$$\mathcal{K}_{d_k}(H_k, g_k) = \text{span}\{g_k, H_k g_k, \dots, (H_k)^{d_k-1} g_k\} = \text{Range}(V_k).$$

By taking advantage of the symmetry of H_k , the basis V_k can be constructed by the Lanczos method [24] which requires a single matrix-vector multiplication with H_k per iteration along with a short-term orthonormalization procedure. Even though the entire basis is not required in this latter step, our *freezing* strategy needs to store it to be able to keep using V_k in later nonlinear iterations. This is in contrast with other contributions like, e.g., [17], where the basis is not stored in the first place but needs to be reconstructed by running a second Lanczos pass to retrieve the final solution.

We would like to stress that in case of polynomial Krylov subspaces, Line 4 in Algorithm 3.2 is redundant. Indeed, whenever a refresh is performed, $\text{span}(g_k) \subseteq \text{Range}(V_k)$ and g_k is orthogonal to the following basis vectors by construction.

We also experimented with different approximation spaces. In particular, in section 6.3.3 we report the results obtained by adopting the *rational* Krylov subspace. While the latter oftentimes attains better numerical performance (see Tables B.2-B.3), rational Krylov subspaces turn out to be competitive on certain, particularly challenging, problems.

6. Computational experiments. In this section we illustrate the performance of our new *freezing* paradigm for the computation of an approximate first-order optimality point. We recall that we are mainly interested in solving optimization problems for which the solution of the regularized Newton linear system by direct methods is both feasible and efficient. Iterative approaches could be an alternative option, but they generally require the employment of preconditioning techniques to achieve competitive performance and strongly rely on the properties of the coefficient matrix at hand. Therefore, in our implementation of FAR2 we employ direct methods for the solution of the regularized Newton system and compare FAR2 against the state-of-the-art implementation of AR2 based on the secular equations and direct solvers. The FAR2 framework is designed for general approximation spaces; in our comparisons we adopt the polynomial Krylov subspace (FAR2-PK), while in section 6.3.3 we also report some results obtained with the rational Krylov subspace as approximation space (FAR2-RK).

6.1. Implementation details. We implemented FAR2, whose details are given in Algorithms 3.1-3.2, in Matlab⁴ [30] and we used the following standard

⁴MATLAB R2019b on a Intel Core i7-9700K CPU @ 3.60GHz x 8, 16 GB RAM, 64-bit.

values for the parameters

$$(6.1) \quad \eta_1 = 0.1, \eta_2 = 0.8, \gamma_1 = 0.1, \gamma_2 = 2, \theta_1 = 0.1, \sigma_{\min} = 10^{-8},$$

along with

$$C_{\text{low}} = 10^{-20}, C_{\text{up}} = 10^{20}.$$

In Step 3.3, in case $\rho_k \geq \eta_2$ we set $\sigma_{k+1} = \gamma_1 \sigma_k$. The maximum subspace dimension is set to $j_{\max} = 50$. Moreover, the solution of the secular equation projected onto $\text{Range}(W_k)$ (Lines 6 and 17 of Algorithm 3.2) is performed by using the Matlab function `fzero` providing

$$[\min(-\lambda_{\min}(H^{(j)}), 0), \min(-\lambda_{\min}(H^{(j)}), 0) + 1000],$$

as starting interval for the bisection method. All the (shifted) linear systems involved in our procedure are solved by the Matlab backslash operator.

In the rare scenario where our predictor-corrector scheme fails, namely Line 11 of Algorithm 3.1 is performed, the step s_k is computed by employing the state-of-the-art solver RQS included in the GALAHAD optimization library (version 2.3)⁵ based, once again, on direct solvers for linear systems. We used the Matlab interface and default parameters except for the values `control.stop_normal` = θ/σ_k in order to fulfill the condition (2.6).

We compare the performance of our new method against a classic implementation of Algorithm 2.1 that makes use of the parameter values in (6.1) and uses RQS in Step 2 equipped with all the default parameters except for the value `control.stop_normal` = θ . We refer to the corresponding overall implementation as AR2-RQS⁶.

All algorithms terminate when one of the following conditions holds:

$$(6.2) \quad \text{(i)} \quad \|g_k\| \leq \epsilon_r \|g_0\|,$$

where $\epsilon_r > 0$ depends on the problem test set⁷; (ii) 5000 iterations are performed; (iii) the computational time limit of 2 hours is reached.

6.2. Test problems. We considered the test problems in the OPM testing set [21], which contains a small collection of CUTEst unconstrained and bound-constrained nonlinear optimization problems. From all the problems listed in [21] we selected the unconstrained ones. For those problems allowing for a variable dimension n , we specify the adopted value of n in Table B.1 in Appendix B.

As testing problems, we also considered binary classification problems. We suppose we have at our disposal a training set of pairs $\{(a_i, b_i)\}$ with $a_i \in \mathbb{R}^n$, $b_i \in \{-1, 1\}$ (or $b_i \in \{0, 1\}$) and $i = 1, \dots, N$, where b_i denotes the correct sample classification. We perform both a logistic regression and a sigmoidal regression, yielding convex and non convex problems, respectively.

In the first case, we consider as training objective function the logistic loss with ℓ_2 regularization [1, 4], i.e.

$$f(x) = \frac{1}{N} \sum_{i=1}^N \log \left(1 + e^{-b_i a_i^T x} \right) + \frac{1}{2N} \|x\|_2^2,$$

⁵Available from <http://galahad.rl.ac.uk/galahad-www/>.

⁶We have also performed experiments employing the parameter value `control.stop_normal` = θ/σ_k , but the corresponding implementation of AR2-RQS was much less robust than using `control.stop_normal` = θ . Therefore, we chose to report the results obtained with the latter value only.

⁷The stopping criterion (6.2) corresponds to setting $\epsilon = \epsilon_r \|g_0\|$ in Algorithms 2.1 and 3.1.

with $b_i \in \{-1, 1\}$. In the second case the following sigmoid function and least-squares loss is employed [2, 31]

$$f(x) = \frac{1}{N} \sum_{i=1}^N \left(b_i - \frac{1}{1 + e^{-a_i^T x}} \right)^2,$$

with $b_i \in \{0, 1\}$. We used the six data sets⁸ reported in Table 6.1 together with the dimension n of the parameter vector $x \in \mathbb{R}^n$.

For OPM and binary classification problems, we ran the algorithms until (6.2) holds with $\epsilon_r = 10^{-6}$ and $\epsilon_r = 10^{-3}$, respectively.

6.3. Numerical results. We compare the performance of FAR2-PK with the state-of-the-art factorization-based AR2 method, labeled as AR2-RQS. To provide sensible insight on the general numerical behaviour of the proposed FAR2 framework, we focus on the number of n -dimensional factorizations and nonlinear iterations performed by the different algorithms.

6.3.1. Results for the OPM test set. The performance profiles related to the OPM problems⁹ listed in Table B.1 are reported in Figure 6.1. We remind the reader that a performance profile graph $p_A(\tau)$ of an algorithm A at point τ shows the fraction of the test set for which the algorithm is able to solve within a factor of τ of the best algorithm for the given measure [12]. Once again, these performance profiles take into account the number of n -dimensional factorizations and nonlinear iterations as performance measures.

The profiles in Figure 6.1 clearly show an outstanding advantage in using our FAR2-PK approach in terms of total number of matrix factorizations with respect to AR2-RQS. Indeed, FAR2-PK is the most efficient routine in 94% of the runs and AR2-RQS is within a factor 2 of FAR2-PK in only 11% of the runs. The behavior of the two routines in terms of number of nonlinear iterations is rather similar, while AR2-RQS is slightly more robust solving one problem more than FAR2-PK¹⁰.

The first two sets of columns in Tables B.2 and B.3 in Appendix B collect the detailed results used to generate the plots in Figure 6.1. In particular, we report the number of nonlinear iterations ($\#NLI$) and the number of n -dimensional factorizations ($\#fact$) for the two solvers and for each problem. In addition, for the FAR2 method the tables include also the number of nonlinear iterations where the space is refreshed ($\#ref$), the average dimension of the projected problems (ave_K), the number of times the step s_k is computed in Line 6 of Algorithm 3.1 ($\#sub$) using a frozen subspace, and the number of times the solver resorts to the secant method in Line 11 of Algorithm 3.1 ($\#sec$). These results provide a good understanding of the general behaviour of our algorithm. First, we observe that the basis refresh is invoked rarely, specifically in the 1.8% of the total number of nonlinear iterations. Second, in the 3.5% of the nonlinear iterations, the step s_k is computed in Line 6, that is condition (2.6) is satisfied avoiding the solution of the linear system in Line 8 thus saving a lot of computational efforts. Third, the results clearly show that the secant method in Line 11 is a mere safeguard step as it is called 0.8% of times by FAR2-PK.

6.3.2. Results for the binary classification problems. Similar results are obtained on the binary classification problems. Table 6.1 collects the results distinguishing between the logistic and the sigmoidal loss function cases for the six

⁸A9A [9], CINA0 [9], GSETTE [9], MNIST [25], MUSH [9], REGERD0 [8]

⁹All the tested algorithms failed in solving the very ill-conditioned problems ARGLINB, ARGLINC, COSINE, GENHUMPS, PENALTY2, and SCOSINE. Therefore, these problems have been excluded from the testing set. Moreover, they all did not converge in 2 hours when trying to solve CHEBYQUAD.

¹⁰The failure occurred because the maximum number of iterations was reached.

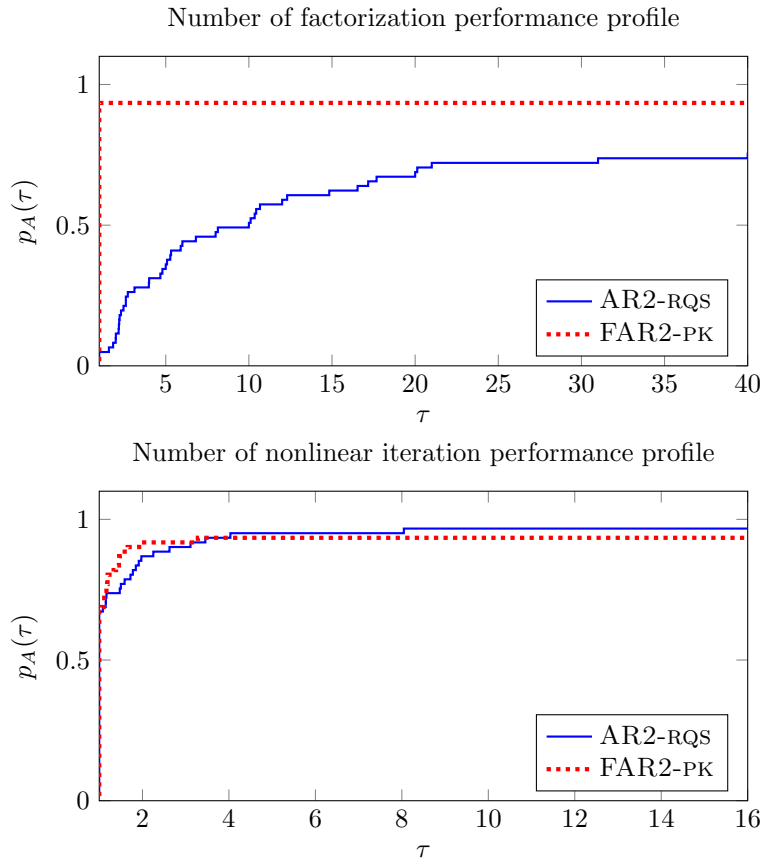


FIG. 6.1. Section 6.3.1. Performance profiles of AR2-RQS and FAR2-PK for the OPM set. Top: Number of factorizations. Bottom: Number of nonlinear iterations.

datasets we tested. In spite of the larger number of nonlinear iterations ($\#NLI$) performed by FAR2-PK in a few cases, we remark that the overall number of factorizations always remains much in favour of FAR2-PK when compared to AR2-RQS. In particular, FAR2-PK is extremely efficient in terms of $\#fact$ while keeping the dimension of the polynomial Krylov subspace rather low.

Figures 6.2-6.3 provide an easier visualization of the behaviour of the two routines we tested in terms of number of factorizations for two reference problems: CINA0 and MNIST. In all cases, we observe that FAR2-PK perform very few factorizations and the subspace-freezing strategy typically leads to a single factorization per nonlinear iteration or even no factorizations at all if the approximate solution $s_k = W_k \hat{s}_k$ to the secular equation satisfies (2.6) in Line 6 of Algorithm 3.1 (see Figures 6.2-6.3). This happens for several nonlinear iterations.

The sigmoidal case of MNIST in Figure 6.3 shows an unusual trend of FAR2-PK where many more nonlinear iterations are performed compared to what happens for AR2-RQS and the regularized Newton step is used frequently. This is probably the worst scenario for FAR2. Indeed, computing the regularized Newton step in many nonlinear iterations can deteriorate the gains coming from our freezing strategy as the number of linear systems to be solved may dramatically increase. Nevertheless, FAR2 is still able to perform a number of factorizations that is much lower than the one needed by AR2-RQS; see Table 6.1.

Finally, we observe that for strictly convex problems, as those obtained by using the logistic loss in classification problems, the refresh strategy is never activated as,

logistic loss	# fact(ave_K)		#NLI	
data set(n)	AR2-RQS	FAR2-PK	AR2-RQS	FAR2-PK
A9A (123)	16	3(2)	7	8
CINA0 (132)	36	1(26)	7	6
GISETTE (5000)	24	1(10)	7	7
MNIST (784)	22	4(4)	8	8
MUSH (112)	20	0(3)	9	19
REGED0 (999)	8	7(50)	8	7

sigmoidal loss	# fact (ave_K)		#NLI	
data set(n)	AR2-RQS	FAR2-PK	AR2-RQS	FAR2-PK
A9A (123)	19	3(2.5)	8	21
CINA0 (132)	49	1(26)	7	6
GISETTE (5000)	58	4(7.6)	9	37
MNIST (784)	116	30(3)	16	39
MUSH (112)	27	0(3)	10	33
REGED0 (999)	14	6(50)	7	6

TABLE 6.1

Section 6.3.2. Results on binary classification problems: number of factorization (# fact) and number of nonlinear iterations (#NLI) for the AR2-RQS and the FAR2-PK methods.

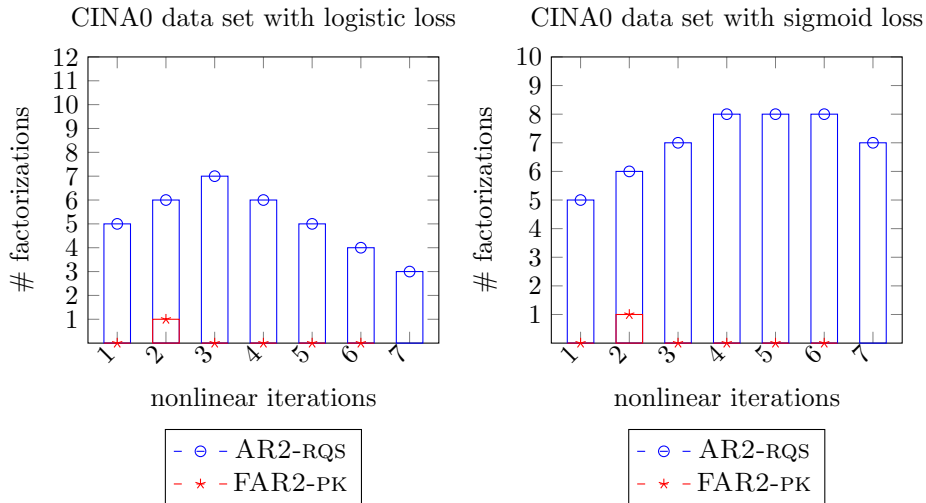


FIG. 6.2. Section 6.3.2. Number of factorizations per nonlinear iteration for the CINA0 data set.

in fact, $H_k + \lambda I$ is positive definite for any $\lambda \geq 0$ and condition (3.2) is always met in practice.

6.3.3. On the use of a different approximation space: a numerical illustration. As already mentioned, our new FAR2 framework is rather flexible and, in principle, any approximation space can be adopted in our solution procedure. In this last experiment we explore the use of rational Krylov subspaces as approximation space. To the best of our knowledge, rational Krylov subspaces have never been proposed in the context of nonlinear optimization prior this work. We thus report additional details about its construction and properties.

Given a suitable set of shifts $z_{d_k} = (\xi_1, \dots, \xi_{d_k}) \in \mathbb{R}^{d_k}$, the rational Krylov subspace of dimension d_k generated by the symmetric matrix H_k and the vector g_k

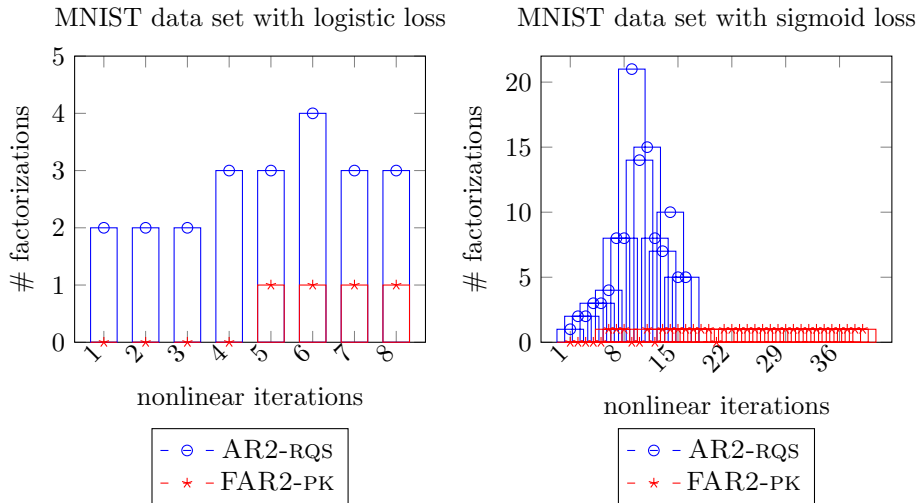


FIG. 6.3. Section 6.3.2. Number of factorizations per nonlinear iteration for the MNIST data set.

is defined as follows¹¹

$$(6.3) \quad \mathcal{K}_{d_k}(H_k, g_k, z_{d_k}) = \text{span} \left\{ (H_k + \xi_1 I)^{-1} g_k, \dots, \prod_{j=1}^{d_k} (H_k + \xi_j I)^{-1} g_k \right\}.$$

An orthonormal basis $V_k \in \mathbb{R}^{n \times d_k}$ of \mathcal{K}_{d_k} can be constructed by means of the rational Arnoldi method [28] or the rational Lanczos scheme [27]. Starting with $v_1 = (H_k + \xi_1 I)^{-1} g_k$, normalized to have unit norm, the next basis vector is obtained by first computing $\tilde{v}_2 = (H_k + \xi_2 I)^{-1} v_1$, orthogonalizing \tilde{v}_2 with respect to the previous vectors, in this case only v_1 , and finally normalizing to have unit norm. The procedure thus continues recursively.

One of the major computational costs per iteration of the rational Krylov subspace basis construction amounts to the solution of a shifted linear system with H_k , especially in case H_k is not very sparse. Therefore, to limit computational costs the number of performed iterations $d_k \leq j_{\max}$ should remain small. To this end, the choice of the shifts is crucial. Quasi-optimal and adaptive procedures have been proposed, where the shifts are computed automatically; see, e.g., [22, 14, 13] and the references therein. In case H_k is semi-definite, as it is expected to occur for large enough k , the nonzero shifts are chosen to have the same signature of H_k so that $H_k + \xi_j I$ results in a positive definite matrix. On the other hand, if H_k is slightly indefinite as it may happen at the beginning of the outer nonlinear procedure, the shifts can be selected to ensure that $H_k + \xi_j I$ is still nonsingular. However, we would like to remark that we never needed to implement special strategies for the singular cases during our extensive experimental testing. In particular, although some instances of $H_k + \xi_j I$ turned out to be ill-conditioned, this aspect did not seem to severely affect the quality of the computed subspace. The adaptive shift selection procedure described in [14] has been adopted to obtain all the numerical results reported in this section.

Rational Krylov spaces are generally able to capture good spectral information on a given problem already for small dimensions, compared to classic polynomial

¹¹For convenience, we do not include g_k in the space definition, following the typical setting in model order reduction. Nonetheless, the vector g_k is included in the projection phase, see Algorithm 3.2.

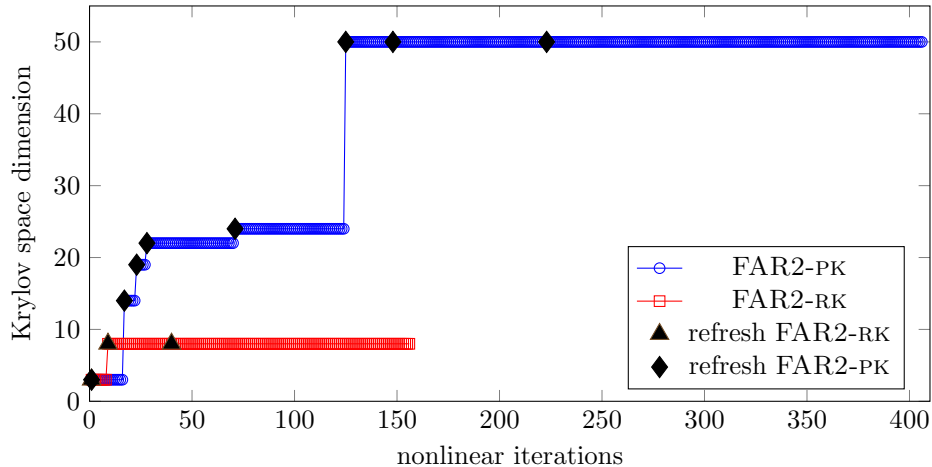


FIG. 6.4. Section 6.3.3. Dimension of the Krylov subspace versus the nonlinear iterations for the EIGENBLS problem in OPM and subspace refresh: FAR2-RK and FAR2-PK.

Krylov subspaces, thus significantly reducing the original problem size. Moreover, we expect the rational Krylov subspace generated by H_k and g_k to still be a successful approximation space for successive nonlinear iterations, especially if the spectral properties of H_k slowly change with k . On the other hand, the rational Krylov basis construction is rather expensive as it requires the solution of linear systems.

In Tables B.2-B.3 we report the results obtained by solving all the OPM problems by FAR2 adopting either the rational Krylov (RK) or the polynomial Krylov (PK) subspace as approximation space. As it can be seen from these results, employing RK very often leads to an overall number of factorizations that is smaller than the one performed by adopting AR2-RQS but, almost always larger than the one required employing PK. We can thus confidently say that PK is often the right choice as approximation space in this regard. However, in case the overall number of outer iterations performed by adopting PK is significantly higher than employing RK, solely looking at the number of factorizations may give only a partial picture of the actual numerical performance of the whole procedure. This is especially the case for sparse problems where the linear system solution cost is proportional to the number of nonzeros of the coefficient matrix [29].

As a representative example, we report in Figure 6.4 the results obtained for the EIGENBLS problem from OPM with $\epsilon_r = 10^{-4}$ in (6.2) for the sake of better readability¹²: for each nonlinear iteration the dimension of the generated Krylov subspace is reported. We also highlight those iterations where a refresh of the Krylov subspace takes place. We can observe that the dimension of the PK subspace reaches the maximum dimension allowed ($j_{\max} = 50$) for large k . This is probably due to the large conditioning of the Hessian matrix which becomes of the order of 10^7 for $k > 100$. Working with a larger subspace implies an increase in the cost of computing the projected step \hat{s}_k in Algorithm 3.2. On the contrary, the dimension of the RK subspace stays always below 8 making the cost of computing \hat{s}_k negligible. Another evident drawback of employing PK in this example is the much larger number of nonlinear iterations we need to perform if compared to the case where RK is adopted. This leads to an increase in the cost of basically every step of our scheme: The projection phase (e.g., the explicit construction of $H^{(j)} = (W^{(j)})^T H_k W^{(j)}$), the regularized Newton step computation, and, more remarkably, the Hessian matrix

¹²We remind the reader that the results in Tables B.2-B.3 are obtained by setting $\epsilon_r = 10^{-6}$. This explains the different values reported in Figure 6.4.

H_k and the gradient g_k evaluation; FAR2-PK carries out all these steps hundreds of times more than FAR2-RK in this example. In particular, for both FAR2-PK and FAR2-RK, constructing H_k and g_k amounts to approximately the 85% of the overall computational time. As a consequence, FAR2-RK turns out to be faster than FAR2-PK in spite of the more expensive basis construction of the former. In particular, in this example, the overall running time of FAR2-RK and FAR2-PK is 86.2 and 233.9 seconds, respectively¹³.

7. Discussion and conclusions. For the practical use of the adaptive regularization method, the efficient minimization of the cubic regularized model is a crucial issue. We have addressed this bottleneck by proposing a new two-step procedure, the FAR2 method. The main difference between FAR2 and standard adaptive-regularization techniques lies in the minimization of the involved model: in FAR2 this minimization is carried out over a possibly frozen subspace. Under standard conditions, we have proved that the optimal worst-case complexity of the original AR2 method is preserved, regardless of the adopted subspace.

Our extended experimental testing shows that the freezing paradigm is able to considerably reduce the overall number of matrix factorizations compared to classic procedures based on the solution of the full space secular equation. In terms of approximation space, we have explored the use of both rational and polynomial Krylov subspaces. While they both lead to a rather successful solution process, the use of FAR2 combined with polynomial Krylov subspaces turns out to be extremely efficient in most cases, whereas the implementation employing rational Krylov subspaces seems a valid alternative especially for sparse problems, where the additional cost coming from linear systems solves involved in the basis construction remains limited.

We finally remark that the proposed approach could be easily adapted to trust-region frameworks with second order models; see, e.g. TR2 in [7, Section 3.2]. Our reduced approach could be appealing whenever the solution of the trust-region subproblem beyond the Steihaug–Toint point is sought; see, e.g., [17, 18]. Indeed, in this case, if the current step lies on the trust-region boundary, the following secular equation

$$\phi_T(\lambda; g_k, H_k, \Delta_k) \stackrel{\text{def}}{=} \|(H_k + \lambda I)^{-1} g_k\| - \Delta_k = 0,$$

has to be (approximately) solved; here $\Delta_k > 0$ is the so-called trust-region radius. Therefore, Algorithm 3.2 can be straightforwardly modified by using ϕ_T in place of ϕ_R in Lines 6 and 17.

Acknowledgments. The work of all the authors was partially supported by INdAM-GNCS under the INdAM-GNCS project CUP_E53C22001930001. The research of S. B. was partially granted by the Italian Ministry of University and Research (MUR) through the PRIN 2022 “Numerical Optimization with Adaptive Accuracy and Applications to Machine Learning”, code: 2022N3ZNAX MUR D.D. financing decree n. 973 of 30th June 2023 (CUP B53D23012670006). The research of S. B. and M. P. was partially granted by PNRR - Missione 4 Istruzione e Ricerca - Componente C2 Investimento 1.1, Fondo per il Programma Nazionale di Ricerca e Progetti di Rilevante Interesse Nazionale (PRIN) funded by the European Commission under the NextGeneration EU programme, project “Advanced optimization METHODS for automated central vein Sign detection in multiple sclerosis from magnetic resonance imaging (AMETISTA)”, code: P2022J9SNP, MUR D.D. financing decree n. 1379 of 1st September 2023 (CUP E53D23017980001). The work of D. P. and V. S. was partially supported by the European Union - NextGenerationEU under the National Recovery and Resilience Plan (PNRR) - Mission 4 Education and research - Component 2 From research to business - Investment 1.1 Notice Prin 2022 - DD N. 104 of 2/2/2022,

¹³For illustrative purposes only, we report that AR2-RQS that uses optimized and compiled functions written in Fortran, takes 517.8 seconds for the EIGENBLS problem.

Appendix A. The Frozen AR2 algorithm for second order optimality points.

Given $\epsilon, \epsilon_H > 0$, Algorithm 3.1 can be suitably modified in order to compute an (ϵ, ϵ_H) -approximately second-order minimizer (see (1.5)). We will refer to this variant of FAR2 as FAR2-SO (Frozen AR2-Second Order). The corresponding algorithms are detailed in Algorithm A.1 and Algorithm A.2 and the introduced modifications are listed below.

- Once an ϵ -approximate first order optimality point has been reached, in order to obtain further progress towards an approximate second-order optimality point, the stronger condition $H_k + \widehat{\lambda}_k I \succ 0$ is needed to employ the regularized Newton step, rather than (3.1). For the sake of simplicity, in Algorithm A.1 we did not distinguish between iterations where $\|g_k\| > \epsilon$ or $\|g_k\| \leq \epsilon$ and, at any iteration, in Line 9 we replace the condition $s_k^T (H_k + \widehat{\lambda}_k I) s_k \leq 0$ by $H_k + \widehat{\lambda}_k I \not\succeq 0$.
- Algorithm A.1 needs to be equipped with a second-order stopping criterion; in Step 1 the algorithm is stopped whenever the following two conditions hold:

$$(A.1) \quad \|g_k\| \leq \epsilon \quad \text{and} \quad \lambda_{\min}(H_k) \geq -\epsilon_H.$$

- In Line 5 of Algorithm A.1 the following condition has to be checked in addition to (2.6):

$$(A.2) \quad \lambda_{\min}(\nabla^2 m_k(s_k)) \geq -\theta_2 \|s_k\|, \quad \theta_2 > 0.$$

- In Line 11 of Algorithm A.1 (s_k, λ_k) has to satisfy (A.2) in addition to (2.5)-(2.6).
- In Line 8 of Algorithm A.2 the condition $\lambda_{\min}(\nabla^2 m_k(W^{(j)} \hat{s})) \geq -\theta_2 \|\hat{s}\|$ has to be checked, too.

We stress that H_k is expected to be positive definite during the final convergence phase of the FAR2-SO method and this ensures that condition (3.2) holds eventually.

Next, we provide an upper bound on the number of iterations needed by FAR2-SO to compute an (ϵ, ϵ_H) -approximately second-order minimizer.

THEOREM A.1. *Suppose that **AS.1** and **AS.2** hold. Given $\epsilon, \epsilon_H \in (0, 1)$, there exist positive constants κ_p and κ_H such that the FAR2-SO algorithm needs at most*

$$\left[(f(x_0) - f_{\text{low}}) \max \left\{ \frac{\epsilon^{-\frac{3}{2}}}{\kappa_p}, \frac{\epsilon_H^{-2}}{\kappa_H} \right\} + 1 \right],$$

successful iterations and at most

$$\left[(f(x_0) - f_{\text{low}}) \max \left\{ \frac{\epsilon^{-\frac{3}{2}}}{\kappa_p}, \frac{\epsilon_H^{-2}}{\kappa_H} \right\} + 1 \right] \left(3/2 + \frac{3/2 |\log \gamma_1|}{\log \gamma_2} \right) + \frac{3/2}{\log \gamma_2} \log \left(\frac{\sigma_{\max}}{\sigma_0} \right),$$

iterations to compute an iterate x_k such that $\|g_k\| \leq \epsilon$ and $\lambda_{\min}(H_k) \geq -\epsilon_H$.

Proof. Let us keep the same notation of Section 4 and denote with \mathcal{I}_{RN} the set of iteration indexes such that s_k has been computed in Line 8 of Algorithm A.1.

Algorithm A.1 The Frozen AR2 algorithm for second order optimality points (FAR2-SO)

Require: An initial point x_0 ; accuracy thresholds $\epsilon, \epsilon_H \in (0, 1)$; an initial regularization parameter $\sigma_0 > 0$ are given, and constants $\eta_1, \eta_2, \gamma_1, \gamma_2, \theta_1, \theta_2, \sigma_{\min}$ s.t.

$$\sigma_{\min} \in (0, \sigma_0], \theta_1 > 0, \theta_2 > 0, 0 < \eta_1 \leq \eta_2 < 1, \\ 0 < \gamma_1 < 1 < \gamma_2, 0 < C_{\text{low}} < C_{\text{up}}$$

An integer $j_{\max} \ll n$.

- 1: Compute $f(x_0), g_0 = \nabla f(x_0), H_0 = \nabla^2 f(x_0)$, and set $k = 0$, **refresh** = 1 and $V_0 = \square$.
- 2: **Step 1: Test for termination.** If $\|g_k\| \leq \epsilon$ and $\lambda_{\min}(H_k) \geq -\epsilon_H$, terminate.
- 3: **Step 2: Step computation.**
- 4: Invoke Algorithm A.2 providing the scalar $\hat{\lambda}_k$, and the reduced step \hat{s}_k , the basis W_k and V_{k+1}
- 5: **if** $W_k \hat{s}_k$ satisfies (2.6) and (A.2)
- 6: set $s_k = W_k \hat{s}_k$ and **goto** Step 3
- 7: **end if**
- 8: Compute $s_k = -(H_k + \hat{\lambda}_k I)^{-1} g_k$. % regularized Newton step
- 9: **if** $(H_k + \hat{\lambda}_k I) \not\approx 0$ or $\|s_k\|/\|\hat{s}_k\| < C_{\text{low}}$ or $\|s_k\|/\|\hat{s}_k\| > C_{\text{up}}$
- 10: **if refresh**
- 11: Find λ_k and $s_k = -(H_k + \lambda_k I)^{-1} g_k$ such that (2.5)-(2.6), and (A.2) hold by applying the secant method to $\phi_R(\lambda_k; g_k, H_k, \sigma_k) = 0$
- 12: **Goto** Step 3
- 13: **else**
- 14: Define $x_{k+1} = x_k, \sigma_{k+1} = \sigma_k$, set **refresh** = 1, $k = k + 1$
- 15: **Goto** Step 1 % unsuccessful iteration, step rejection
- 16: **end if**
- 17: **Step 3** Compute

$$\rho_k = \frac{f(x_k) - f(x_k + s_k)}{T_k(0) - T_k(s_k)}.$$

- 18: **Step 4**
- 19: **if** $\rho_k \geq \eta_1$ **then** % Successful iteration
- 20: set $x_{k+1} = x_k + s_k$, compute $g_{k+1} = \nabla f(x_{k+1}), H_{k+1} = \nabla^2 f(x_{k+1})$
- 21: **else** % unsuccessful iteration, step rejection
- 22: set $x_{k+1} = x_k$
- 23: **end if**
- 24: **Step 5: Regularization parameter update.** Compute

$$\sigma_{k+1} \in \begin{cases} [\max\{\sigma_{\min}, \gamma_1 \sigma_k\}, \sigma_k] & \text{if } \rho_k \geq \eta_2 \\ \sigma_k & \text{if } \rho_k \in [\eta_1, \eta_2) \\ \gamma_2 \sigma_k & \text{otherwise} \end{cases}$$

- 25: Increment k by one set **refresh** = 0 and **goto** Step 1.
-

Note that at any successful iteration k in such a set, it must hold that $H_k + \hat{\lambda}I$ is positive definite. Then,

$$\lambda_{\min}(H_k) > -\hat{\lambda}.$$

Therefore, by using **AS.1** and Lemma 3.3, for any successful iteration k with $k \in$

Algorithm A.2 Minimization of m_k over the low-dimensional subspace

(second order optimality case)

Require: The matrix H_k ; the vector g_k ; the matrix $V_k \in \mathbb{R}^{n \times d_k}$; accuracy thresholds $\theta_1 > 0$, $\theta_2 > 0$; the parameter σ_k ; an integer $j_{\max} \ll n$; **refresh**.

```
1:   if refresh                                     % Generate new proj space
2:     Set  $V_{k+1} = []$ 
3:     for  $j = 1, \dots, j_{\max} - 1$ 
4:       Set  $W^{(j)} = \text{orth}([V_{k+1}, g_k])$ 
5:       Compute projections  $g^{(j)} = (W^{(j)})^T g_k$ ,    $H^{(j)} = (W^{(j)})^T H_k W^{(j)}$ 
6:       Find  $\hat{\lambda}$  s.t.  $\phi_R(\hat{\lambda}; g^{(j)}, H^{(j)}, \sigma_k) = 0$ , i.e.
                                     
$$\hat{\lambda} = \sigma_k \|(H^{(j)} + \hat{\lambda}I)^{-1} g^{(j)}\|$$

7:       Set  $\hat{s} = -(H^{(j)} + \hat{\lambda}I)^{-1} g^{(j)}$ 
8:       if  $\|\nabla m_k(W^{(j)} \hat{s})\| \leq \frac{1}{2} \theta_1 \|\hat{s}\|^2$  and
                                     
$$\lambda_{\min}(\nabla^2 m_k(W^{(j)} \hat{s})) \geq -\theta_2 \|\hat{s}\|$$

9:         Set  $\hat{\lambda}_k = \hat{\lambda}$ ,  $\hat{s}_k = \hat{s}$ ,  $W_k = W^{(j)}$  and return
10:      end if
11:      Expand  $V_{k+1}$  with new Krylov direction
12:    end for
13:    Set  $\hat{\lambda}_k = \hat{\lambda}$ ,  $\hat{s}_k = \hat{s}$ ,  $W_k = W^{(j)}$  and return
14:  else                                           % Project onto the old space
15:    Set  $W^{(\hat{j})} = \text{orth}([V_k, g_k])$ , where  $\hat{j} = d_k + 1$ 
16:    Compute projections  $g^{(\hat{j})} = (W^{(\hat{j})})^T g_k$ ,    $H^{(\hat{j})} = (W^{(\hat{j})})^T H_k W^{(\hat{j})}$ 
17:    Find  $\hat{\lambda}$  s.t.  $\phi_R(\hat{\lambda}; g^{(\hat{j})}, H^{(\hat{j})}, \sigma_k) = 0$ , i.e.
                                     
$$\hat{\lambda} = \sigma_k \|(H^{(\hat{j})} + \hat{\lambda}I)^{-1} g^{(\hat{j})}\|$$

18:    Set  $\hat{s}_k = -(H^{(\hat{j})} + \hat{\lambda}I)^{-1} g^{(\hat{j})}$ ,    $\hat{\lambda}_k = \hat{\lambda}$ 
19:    Set  $V_{k+1} = V_k$  and  $W_k = W^{(\hat{j})}$ 
20:  end if
```

 \mathcal{I}_{RN} and for any $d \in \mathbb{R}^n$, $\|d\| = 1$, we obtain

$$\begin{aligned} d^T H_{k+1} d &= d^T (H_{k+1} - H_k) d + d^T H_k d \geq -L_2 \|s_k\| - \hat{\lambda} \\ &= -L_2 C_{\text{up}} \|\hat{s}_k\| - \sigma_k \|\hat{s}_k\| \geq -(L_2 C_{\text{up}} + \sigma_{\max}) \|\hat{s}_k\|. \end{aligned}$$

This latter inequality, along with $\min_{\|d\|=1} d^T H_{k+1} = \lambda_{\min}(H_{k+1})$ and Lemma 4.3, yields

$$(A.3) \quad \|\hat{s}_k\| \geq \max\{\kappa_0^{1/3} \|g_{k+1}\|^{1/2}, -\kappa_{H,0}^{1/3} \lambda_{\min}(H_{k+1})\},$$

where $\kappa_{H,0} = \left(\frac{1}{L_H C_{\text{up}} + \sigma_{\max}}\right)^3$ and κ_0 has been defined as in Lemma 4.3. Moreover, by (4.2)

$$f(x_k) - f(x_{k+1}) \geq \eta_1 (T_k(0) - T_k(s_k)) \geq \frac{\eta_1}{2} \sigma_k \|\hat{s}_k\| \|s_k\|^2 \geq \frac{\eta_1}{2} \sigma_{\min} C_{\text{low}}^2 \|\hat{s}_k\|^3,$$

and we can conclude that for any successful iteration k with $k \in \mathcal{I}_{RN}$ it holds

$$f(x_k) - f(x_{k+1}) \geq \frac{\eta_1}{2} \sigma_{\min} C_{\text{low}}^2 \max\{\kappa_0 \|g_{k+1}\|^{3/2}, -\kappa_{H,0} \lambda_{\min}(H_{k+1})\}^3.$$

Problem	n	Problem	n	Problem	n	Problem	n
ARGLINA	1000	DIXMAANC	3000	ENGVAL1	1000	PENALTY3	1000
ARGLINB	1000	DIXMAAND	3000	ENGVAL2	1000	POWELLSSG	1000
ARGLINC	1000	DIXMAANE	3000	EXTROSNB	1000	POWER	1000
ARGTRIG	1000	DIXMAANF	3000	FMINSURF	900	ROSENBR	1000
ARWHEAD	1000	DIXMAANG	3000	FREUROTH	1000	SCOSINE	1000
BDARWHD	1000	DIXMAANH	3000	GENHUMPS	1000	SCURLY10	1000
BROWNAL	1000	DIXMAANI	3000	HELIX	1000	SCURLY20	1000
BROYDENBD	1000	DIXMAANJ	3000	HILBERT	1000	SCURLY30	1000
CHANDHEU	1000	DIXMAANK	3000	INDEF	1000	SENSORS	1000
CHEBYQAD	1000	DIXMAANL	3000	INTEGREQ	1000	SPMSQRT	1000
COSINE	1000	DIXON	1000	MANCINO	1000	TQUARTIC	1000
CRGLVY	1000	DQRTIC	1000	MSQRTALS	900	TRIDIA	1000
CUBE	1000	EDENSCH	1000	MSQRTBLS	900	VARDIM	1000
CURLY10	1000	EG2	1000	NONDIA	1000	WMSQRTALS	900
CURLY20	1000	EG2S	1000	NONDQUAR	1000	WMSQRTBLS	900
CURLY30	1000	EIGENALS	1056	NZF1	1300	WOODS	1000
DIXMAANA	3000	EIGENBLS	1056	PENALTY1	1000		
DIXMAANB	3000	EIGENCLS	1056	PENALTY2	1000		

TABLE B.1

The OPM test problems and their dimension.

In case $k \notin \mathcal{I}_{RN}$, Lemma 3.3.3 in [7] ensures that the step s_k computed in Line 6 of Algorithm A.1 satisfies:

$$\|s_k\| \geq -\frac{1}{L_H + \theta_2 + \sigma_{\max}} \lambda_{\min}(H_{k+1}).$$

Then, from (4.3) and Lemma 4.3 it follows that

$$\begin{aligned} f(x_k) - f(x_{k+1}) &\geq \eta_1(T_k(0) - T_k(s_k)) \geq \frac{\eta_1}{3} \sigma_k \|s_k\|^3 \\ &\geq \frac{\eta_1}{3} \sigma_{\min} \max \left\{ \kappa_1 \|g_{k+1}\|^{3/2}, -\kappa_{H,1} \lambda_{\min}(H_{k+1})^3 \right\}, \end{aligned}$$

where $\kappa_{H,1} = \left(\frac{1}{L_H + \theta_2 + \sigma_{\max}} \right)^{1/3}$.

Finally, for any iteration k such that the FAR2-SO algorithm has not terminated before or at iteration $k + 1$, we must have that either $\|g_{k+1}\| > \epsilon$ or $\lambda_{\min}(H_{k+1}) < -\epsilon_H$. Therefore, at any successful iteration k we have

$$f(x_k) - f(x_{k+1}) \geq \eta_1 \sigma_{\min} \min \left\{ \kappa_p \epsilon^{3/2}, \kappa_H \epsilon_H^3 \right\},$$

with $\kappa_p = \eta_1 \sigma_{\min} \min \left\{ C_{\text{low}}^2 \frac{\kappa_0}{2}, \frac{\kappa_1}{3} \right\}$ and $\kappa_H = \eta_1 \sigma_{\min} \min \left\{ C_{\text{low}}^2 \frac{\kappa_{H,0}}{2}, \frac{\kappa_{H,1}}{3} \right\}$. The thesis then follows proceeding as in the proof of Theorem 4.5. \square

Appendix B. The OPM test set and complete results. We report in Table B.1 the OPM test problems used in the experiments described in section 6.3.1 and their dimension. Tables B.2 and B.3 show the results obtained by using AR2-RQS, FAR2-RK and FAR2-PK in the solution of the OPM problems listed in Table B.1. The tables display the number of nonlinear iterations (#NLI) along with the number of factorizations (#fact) for the three solvers. Moreover, in case of FAR2-RK and FAR2-PK, they report also the number of iterations where the basis is refreshed (#ref), the average dimension of the projected problems (ave_K), the number of times the step s_k is computed in Line 6 of Algorithm 3.1 (#sub) using a frozen subspace, and the number of times the solvers employ the secant method in Line 11 of Algorithm 3.1 (#sec). The symbol '*' means that the nonlinear solver did not converge in 5000 iterations.

	AR2-RQS		FAR2-RK						FAR2-PK					
	#NLI	#fact	#NLI	#fact	# ref	ave_K	#sub	#sec	#NLI	#fact	#ref	ave_K	#sub	#sec
ARGLINA	5	5	5	1	1	1	4	0	5	0	1	1	4	0
ARGTRIG	12	24	12	14	1	3	0	0	12	11	1	17	0	0
ARWHEAD	5	8	5	2	1	2	4	0	5	0	1	2	4	0
BDARWHD	12	24	12	2	1	2	11	0	12	0	1	2	11	0
BROWNAL	2	4	2	2	1	1	0	0	2	0	1	1	1	0
BROYDENBD	7	11	7	9	1	3	0	0	7	6	1	3	0	0
CHANDHEU	2	2	2	2	1	2	1	0	2	0	1	2	1	0
CRGLVY	11	22	12	12	1	2	1	0	13	10	1	2	2	0
CUBE	47	161	47	25	1	3	24	0	47	8	1	10	38	0
CURLY10	23	109	21	77	2	40.7	2	1	20	16	3	20.5	1	0
CURLY20	24	118	25	92	3	43.2	3	1	24	20	3	24	1	0
CURLY30	26	133	31	166	4	43.9	1	2	29	25	3	21.7	1	0
DIXMAANA	6	10	8	2	1	1	6	0	8	1	1	1	6	0
DIXMAANB	38	161	57	58	2	2.1	2	0	11	2	1	2	8	0
DIXMAANC	21	66	8	3	1	2	6	0	8	1	1	2	6	0
DIXMAAND	28	129	42	41	1	2	2	0	9	1	1	2	7	0
DIXMAANE	10	31	10	3	1	2	8	0	10	1	1	2	8	0
DIXMAANF	75	320	64	76	2	11.2	2	0	38	30	1	2	7	0
DIXMAANG	67	395	69	54	1	2	16	0	35	23	2	2.2	10	0
DIXMAANH	73	334	54	53	2	2.6	5	0	46	32	1	2	13	0
DIXMAANI	12	42	21	12	1	2	10	0	14	2	1	2	11	0
DIXMAANJ	81	430	69	57	2	2.2	15	0	36	26	1	2	9	0
DIXMAANK	59	369	77	66	3	2.2	15	0	40	30	1	2	9	0
DIXMAANL	93	445	53	52	1	2	2	0	54	43	2	2.4	9	0
DIXON	9	32	6	7	1	3	1	0	6	4	1	4	1	0
DQRTIC	8	8	8	1	1	1	7	0	8	0	1	0	7	0
EDENSCH	24	89	13	8	1	2	6	0	13	6	1	2	6	0
EG2	16	32	9	1	1	1	8	0	9	0	1	1	8	0
EG2S	68	207	72	61	2	3.7	14	0	99	93	2	3.8	4	0
EIGENALS	523	5309	89	97	1	10	1	0	65	61	1	8	3	0
EIGENBLS	670	2289	847	894	8	6.9	0	0	739	734	9	45.0	0	4

TABLE B.2

Complete results obtained by AR2-RQS FAR2-RK and FAR2-PK on OPM problems in Table B.1.

	AR2-RQS		FAR2-RK						FAR2-PK					
	#NLI	#fact	#NLI	#fact	# ref	ave_K	#sub	#sec	#NLI	#fact	#ref	ave_K	#sub	#sec
EIGENCLS	768	6398	1016	1048	3	15.6	4	0	1273	1260	3	49.4	11	1
ENGVAL1	8	13	8	6	1	1	2	0	8	5	1	1	2	0
EXTROSNB	10	18	10	12	1	3	0	0	10	9	1	6	0	0
FMINSURF	94	211	92	88	1	3	6	0	112	106	1	4	5	0
FREUROTH	6	13	6	7	1	2	0	0	6	5	1	2	0	0
HELIX	17	60	17	17	1	2	1	0	17	10	1	2	6	0
HILBERT	6	12	7	2	1	1	5	0	7	1	1	1	5	0
INDEF	19	93	51	35	3	3.1	25	0	196	55	13	2.3	128	0
INTEGREQ	15	30	13	16	1	4	0	0	13	13	1	50	0	1
MANCINO	121	884	30	555	11	46	0	8	30	50	11	46.5	0	9
MSQRTALS	241	2526	412	625	23	8.6	6	0	256	250	16	45.7	2	12
MSQRTBLS	318	3945	421	774	41	11	14	0	468	485	31	47	2	29
NONDIA	38	83	38	2	1	2	37	0	38	0	1	2	37	0
NONDQUAR	12	58	12	18	1	7	0	0	12	11	1	11	0	0
NZF1	10	20	10	8	1	3	4	0	10	5	1	9	4	0
PENALTY1	14	28	12	1	1	1	11	0	12	0	1	1	11	0
PENALTY3	838	3296	773	835	6	8.4	3	0	75	69	6	35.5	3	3
POWELLSG	12	31	12	4	1	3	10	0	12	0	1	3	11	0
POWR	13	26	12	11	1	11	11	0	12	12	1	50	0	1
ROSENBR	3851	7269	4617	4619	1	3	0	0	4596	4595	1	6	0	0
SENSORS	54	318	61	232	5	29	0	2	79	68	4	22.6	7	0
SPMSQRT	18	59	18	24	2	4.4	1	0	25	24	1	4	0	0
TQUARTIC	12	24	12	9	1	4	6	0	12	5	1	32	6	0
TRIDIA	5	10	5	4	1	2	2	0	5	2	1	2	2	0
VARDIM	24	252	*	*	*	*	*	*	*	*	*	*	*	*
WMSQRTALS	89	761	293	393	12	7.9	2	0	292	280	18	47.3	3	9
WMSQRTBLS	183	1387	240	345	13	10.5	3	0	352	348	7	46.1	2	5
WOODS	15	91	15	4	1	4	14	0	15	0	1	4	14	0

TABLE B.3
Complete results obtained by AR2-RQS FAR2-RK and FAR2-PK on OPM problems in Table B.1. (continued)

- [1] S. BELLAVIA, N. KREJIĆ, AND N. KRKLEČ JERINKIĆ, *Subsampled inexact Newton methods for minimizing large sums of convex functions*, IMA Journal of Numerical Analysis, 40 (2019), pp. 2309–2341.
- [2] S. BELLAVIA, N. KREJIĆ, B. MORINI, AND S. REBEGOLDI, *A stochastic first-order trust-region method with inexact restoration for finite-sum minimization*, Computational Optimization and Applications, 84 (2023), pp. 53–84.
- [3] E. G. BIRGIN AND J. M. MARTÍNEZ, *The use of quadratic regularization with a cubic descent condition for unconstrained optimization*, SIAM Journal on Optimization, 27 (2017), pp. 1049–1074.
- [4] R. BOLLAPRAGADA, R. H. BYRD, AND J. NOCEDAL, *Exact and inexact subsampled Newton methods for optimization*, IMA Journal of Numerical Analysis, 39 (2018), pp. 545–578.
- [5] Y. CARMON AND J. DUCHI, *Gradient Descent Finds the Cubic-Regularized Nonconvex Newton Step*, SIAM Journal on Optimization, 29 (2019), pp. 2146–2178.
- [6] C. CARTIS, N. GOULD, AND P. TOINT, *Trust-region and other regularisations of linear least-squares problems*, BIT Numerical Mathematics, 49 (2009), pp. 21–53.
- [7] C. CARTIS, N. I. M. GOULD, AND P. L. TOINT, *Evaluation complexity of algorithms for nonconvex optimization*, MOS-SIAM Series on Optimization, 2022.
- [8] C.-C. CHANG AND C.-J. LIN, *LIBSVM: A library for support vector machines*, ACM Transactions on Intelligent Systems and Technology, 2 (2011), pp. 27:1–27:27. Software available at <http://www.csie.ntu.edu.tw/~cjlin/libsvm>.
- [9] ———, *UCI machine learning repository*, 2013. <https://archive.ics.uci.edu/ml/index.php>.
- [10] F. E. CURTIS, D. P. ROBINSON, AND M. SAMADI, *A trust region algorithm with a worst-case iteration complexity of $\mathcal{O}(\epsilon^{-3/2})$ for nonconvex optimization*, Mathematical Programming, 162 (2017), pp. 1–32.
- [11] ———, *An inexact regularized Newton framework with a worst-case iteration complexity of for nonconvex optimization*, IMA Journal of Numerical Analysis, 39 (2019), pp. 1296–1327.
- [12] E. D. DOLAN AND J. J. MORÉ, *Benchmarking optimization software with performance profiles*, Mathematical Programming, 91 (2002), pp. 201–213.
- [13] V. DRUSKIN, C. LIEBERMAN, AND M. ZASLAVSKY, *On Adaptive Choice of Shifts in Rational Krylov Subspace Reduction of Evolutionary Problems*, SIAM J. Sci. Comput., 32 (2010), pp. 2485–2496.
- [14] V. DRUSKIN AND V. SIMONCINI, *Adaptive Rational Krylov Subspaces for Large-scale Dynamical Systems*, Systems Control Lett., 60 (2011), pp. 546–560.
- [15] J.-P. DUSSAULT AND D. ORBAN, *Scalable adaptive cubic regularization methods*, Mathematical Programming, (2023), pp. 1–35.
- [16] N. GOULD, D. ROBINSON, AND H. THORNE, *On solving trust-region and other regularised subproblems in optimization*, Mathematical Programming Computation, 2 (2010), pp. 21–57.
- [17] N. I. GOULD, S. LUCIDI, M. ROMA, AND P. L. TOINT, *Solving the trust-region subproblem using the lanczos method*, SIAM Journal on Optimization, 9 (1999), pp. 504–525.
- [18] N. I. GOULD, M. PORCELLI, AND P. L. TOINT, *Updating the regularization parameter in the adaptive cubic regularization algorithm*, Computational Optimization and Applications, 53 (2012), pp. 1–22.
- [19] N. I. GOULD AND V. SIMONCINI, *Error estimates for iterative algorithms for minimizing regularized quadratic subproblems*, Optimization Methods and Software, 35 (2020), pp. 304–328.
- [20] S. GRATTON, S. JERAD, AND P. L. TOINT, *Yet another fast variant of Newton’s method for nonconvex optimization*, arXiv preprint arXiv: 2302.10065, (2023).
- [21] S. GRATTON AND P. L. TOINT, *OPM, a collection of Optimization Problems in Matlab*, arXiv preprint arXiv: 2112.05636, (2021).
- [22] S. GÜTTEL, *Rational Krylov Approximation of Matrix Functions: Numerical Methods and Optimal Pole Selection*, GAMM-Mitteilungen, 36 (2013), pp. 8–31.
- [23] X. JIA, X. LIANG, C. SHEN, AND L.-H. ZHANG, *Solving the cubic regularization model by a nested restarting Lanczos method*, SIAM Journal on Matrix Analysis and Applications, 43 (2022), pp. 812–839.
- [24] C. LANCZOS, *Solution of Linear Equations by Minimized Iterations*, J. Res. Natl. Bur. Stand., 49 (1952), pp. 33–53.
- [25] Y. LECUN, L. BOTTOU, Y. BENGIO, AND P. HAFFNER, *Gradient-based learning applied to document recognition*, Proceedings of the IEEE, 86 (1998), pp. 2278–2324. MNIST database available at <http://yann.lecun.com/exdb/mnist>.
- [26] F. LIEDER, *Solving large-scale cubic regularization by a generalized eigenvalue problem*, SIAM Journal on Optimization, 30 (2020), pp. 3345–3358.
- [27] D. PALITTA, S. POZZA, AND V. SIMONCINI, *The Short-Term Rational Lanczos Method and Applications*, SIAM Journal on Scientific Computing, 44 (2022), pp. A2843–A2870.
- [28] A. RUHE, *The rational Krylov algorithm for nonsymmetric eigenvalue problems. III: Complex shifts for real matrices*, BIT, 34 (1994), pp. 165–176.

- [29] J. SCOTT AND M. TUMA, *Algorithms for Sparse Linear Systems*, Birkhäuser Cham, 2023.
- [30] THE MATHWORKS INC., *MATLAB version: 9.7.0 (R2019b)*, 2019.
- [31] Z. YAO, P. XU, F. ROOSTA, AND M. W. MAHONEY, *Inexact Nonconvex Newton-Type Methods*, INFORMS Journal on Optimization, 3 (2021), pp. 154–182.